Investigating the Occurrence of Hierarchies of Cyclicity in Platform Carbonates

D.A. Pollitt[1*], P.M. Burgess[2] and V.P. Wright[3]

[1] Chevron Corporation, 1500 Louisiana St., Houston, TX. 77018, USA.

[2] Department of Earth Sciences, Royal Holloway University of London, Egham, Surrey, TW20 0EX, UK.

[3] Department of Geology, National Museum of Wales, Cardiff, Cathays Park, Cardiff, CF10 3NP, UK.

*Corresponding author (e-mail: david.pollitt@chevron.com)

7379 words, 19 Figures, 1 Table

Running header: Hierarchies of Cyclicity in Carbonates

Keywords: Carbonates, cyclicity, hierarchy, ice-house

Abstract

Hierarchies of cyclicity have been described from a wide variety of carbonate platform strata, and are assumed to be a consequence of Milkanvotich-forced variations in accommodation, although descriptions of hierarchical strata, including 'cycles' and what they constitute, are typically qualitative, subjective, and in some cases difficult to reproduce. One reason for this is the lack of any detailed definition of what constitutes a hierarchy, as well as the implicit and largely untested nature of the assumptions underpinning most interpretations of hierarchical strata.

In this study we aim to investigate the response of depositional systems if they were to behave in the way implied by sequence stratigraphic (hierarchical) models, to clearly state the assumptions of these models and illustrate the consequences of these assumptions when they are employed in a simple, internally-consistent forward model with plausible parameters.

We define hierarchies, in both the time-domain (chronostratigraphic) and thickness-domain (stratigraphic), as two or more high-frequency sequences in which there exists a repeated trend of decreasing high-frequency sequence (HFS) thickness such that within a single low-frequency sequence (LFS) each high-frequency sequence is thinner than the previous sequence.

Based on this definition, results from 110,000 numerical model runs suggest that ordered forcing via cyclical eustatic sea-level oscillations rarely results in an easily identifiable hierarchy of stacked cycles. Hierarchies measured in the chronostratigraphic time-domain occur in only 9% of model run cases, and in 15% of cases when measured in the thickness-domain, suggesting that vertical thickness trends are probably not a useful way to identify products of ordered periodic external forcing. Variability in relative forcing periodicity results in significant variation in both HFS and LFS thickness trends making accurate identification of hierarchy and any forcing controls from thickness data alone very difficult. Comparison between model results and outcrop sections suggests that hierarchies are often assumed to be present despite a lack of adequate supporting evidence and quantitative analysis of these sections suggests that they are not hierarchical in any meaningful sense.

Introduction

Platform carbonates are important recorders of climatic and tectonic history and form hydrocarbon reservoirs in many basins (e.g. Saller *et al.* 1994). During ice-house periods of global climate platform interior strata are typically characterised by stacked high-frequency sequences (HFSs) that often show clear evidence for high-frequency high-amplitude relative sea-level oscillations (Goldhammer *et al.* 1990). HFSs deposited during ice-house periods are typically defined as a shallowing-upward sequence of sub-tidal strata capped by sub-aerial exposure (Rankey 2004). Individual HFSs are interpreted as 'stacking' into thicker low-frequency sequences (LFSs). LFSs are themselves therefore unconformity bounded packages of strata, following the standard definition of sequence, and are often identified by a vertical trend of decreasing HFS thickness (e.g. Lehrmann and Goldhammer 1999; Kenter *et al.* 2006). These trends, based on variations of facies and thickness, form the basis for identification of a hierarchy of stacked cycles or sequences (Figure 1).

Sedimentary hierarchies are potentially important because, if present, they allow systematic subdivision of strata and also because implicit in hierarchy interpretation is an assumption that it was generated by an ordered forcing-mechanism. The control is typically assumed to be periodic variations in accommodation usually attributed to climate variations resulting from Milankovitch-scale orbital variations (e.g. Cozzi *et al.* 2005; Schwarzacher 2005; Algeo and Hinnov 2006), which vary global sea-level primarily by dictating the amount of water stored as continental ice. The accommodation changes are therefore inferred to be periodic creating a sedimentary hierarchy via interaction of various wavelengths of Milankovitch oscillations (for a review see de Boer and Smith 1994). Hierarchies also have additional implications related to order and completeness of the stratigraphic record, the assumption being that since an ordered forcing mechanism is present in the climate system the stratigraphic record preserves this signal with sufficient fidelity and without significant loss so as to be recognizable. This signal is demonstrably recorded in deep marine settings which undergo almost continuous pelagic sedimentation (e.g. Zachos *et al.* 2001) but less obvious in shallow marine settings which contain presumably significant periods hiatus (as much as 80% of the total depositional period; Barnett *et al*., 2002).

Despite being such a potentially useful concept and approach, a critical problem with interpretation of sedimentary hierarchies to date is the lack of an agreed, detailed definition for the term. A lack of a rigorous definition allows interpretation of hierarchical strata without sufficient evidence to support the resulting conclusions about controlling factors (e.g. Kerans *et al.* 1994), makes objective comparison of proposed examples more difficult, and limits the degree to which hierarchies can be understood.

In this study we aim to investigate the response of depositional systems if they were to behave in the way implied by sequence stratigraphic (hierarchical) models, to clearly state the assumptions of these models and illustrate the consequences of these assumptions when they are employed in an internally-consistent forward model with plausible parameters. We also critically examine the conditions necessary to generate a sedimentary hierarchy and propose a definition for the term as well as a new objective method for quantifying the degree of hierarchy displayed in a sedimentary section. We apply this method to both numerical models of carbonate accumulation and outcrop data in order to determine the likely frequency of occurrence of hierarchical strata in the ancient record, and use this analysis to comment on fidelity of carbonate platform strata as a recorder of external forcing.

Previous definitions of sedimentary hierarchies

Strata can be interpreted to be hierarchical despite the lack of a clear definition, although only in a subjective and qualitative way. Different qualitative definitions implied by various authors prevent consensus, decrease reproducibility and inhibit testing for presence of hierarchical strata (*cf.* Goldhammer *et al.* 1991; Drummond and Wilkinson 1993a; Lerat *et al.* 2000). For example, two distinct sedimentary hierarchies were described from the same sedimentary sections (in the

Paradox Basin, southeastern Utah) by Goldhammer *et al.* (1991) and Lerat *et al.* (2000) but differ significantly. In order to establish a “cycle hierarchy”, Lerat *et al.* state that the criteria rest not on thickness but on the “extent of changes in the depositional environments recorded within a cycle” and “the importance of the cycle bounding surfaces in regional correlations” (Lerat *et al.* 2000; p78). Following from this they state that a “5th-order cycle” or “genetic unit” is defined by a “cyclic but minor change in bathymetry or accommodation as deduced from facies”, and is “the expression of a short term cyclic variation of relative sea-level”. “4th-order sequences”, in contrast, are said to represent “major changes in bathymetry or accommodation”. There are numerous problems with these interpretations given the possibility of complex and incomplete strata (Burgess and Wright 2003; Rankey 2004; Burgess 2006), the lack of strong evidence for ordered strata in many cases (Drummond and Wilkinson 1996; Wilkinson *et al.* 1996; Wilkinson *et al.* 1997; Wilkinson *et al.* 1998), and the evidence against simple lithology and depth relations for shallow-water facies (Rankey 2004). The uncertainty in using “minor bathymetric changes” to define cycle boundaries is therefore clearly problematic and boundaries of a HFS should therefore only be interpreted where there is unambiguous evidence of change in relative sea-level. In shallow-marine settings, due to non-unique facies-depth relations this dictates the use of sub-aerial exposure as bounding events for cycles.

Deriving information on sea-level history from exposure surfaces is, however, difficult because the nature and degree of development of subaerial exposure surfaces varies greatly (e.g. Davies 1991; Vanstone 1998; Sattler *et al.* 2005) and limits the ability to quantify the nature of exposure periods using sedimentary features (Budd *et al.* 2002). Goldhammer *et al.* (1991; 1994) used HFS thickness trends to define a sedimentary hierarchy, providing a clear example of what a hierarchy is interpreted to constitute. Based on observations of variations in cycle thickness throughout a sequence, a hierarchy was interpreted from the relative position of thicker and thinner “fifth-order” high-frequency sequences within a “lower-order” sequence (Goldhammer *et al.* 1991). Fifth-order cycles were interpreted, measured and were found to thin upwards within a succession. When a fifth-order cycle that was thicker than the underlying cycle was observed, it was considered to be the end of that particular sequence and the start of a new lower-frequency sequence (“fourth-order”). From this kind of analysis, “bundles” of cycles in the form of HFS are said to occur within each lower-frequency sequence, with a bundling ratio defined based on how many HFSs occur within the LFS. This ‘cycle-bundling’ concept is now commonly advocated by workers as evidence for the operation of Milankovitch-forced glacio-eustasy. In the case of the Paradox Basin strata, cycle-bundling is manifest at a maximum ratio of 9:1 (with a minimum of 3:1), contrasting with the usual 5:1 ratio quoted for many successions (e.g. Goldhammer *et al.* 1987). A shortfall in the number of high-frequency sequences per sequence is usually accounted for by citing "missed beats" as a cause (*sensu* Goldhammer *et al.* 1994; p262), although it is notable that authors rarely explain how more beats than the usual 5:1 (e.g. the 9:1 described above) are accounted for via this method.

Further examples of more rigorous definitions of hierarchies come from studies critical of interpretations of order in carbonate successions (Drummond and Wilkinson 1993a; 1993b; Wilkinson *et al.* 1997). Drummond and Wilkinson (1993b; p688) state that "…many cyclic sequences exhibit a distinct stacking hierarchy wherein a pattern of thickness is repeated throughout an individual sequence". Drummond and Wilkinson (1993a; p369) expand upon this: "Explicit in this argument is that each meter-scale cycle represents a single excursion of sea-level and that repeated patterns in cycle thickness faithfully represent the constructive interference of forcing functions of different frequency". These statements further reiterate the concept that thickness of cycles bears direct relation to the order of forcing, and that trends in thickness are related to interference of multiple orders of forcing.

An objective definition of a sedimentary hierarchy

These common themes in previous descriptions of sedimentary hierarchies can be used to formulate a more rigorous definition. Since cycle development can be complex (Burgess 2006) and lithofacies are not uniquely diagnostic over shallow-water depth ranges (Rankey 2004), any cyclicity and hierarchies defined using facies transitions must include significant uncertainty. In this study we therefore focus on hierarchies defined in terms of thickness. Hierarchies described in other studies tend to include the following:

(a) The assumption that an ordered forcing-mechanism causes an ordered pattern to be recorded in sedimentary strata by influencing accommodation;
(b) The observation that two or more smaller HFSs "stack" or bundle into a larger LFS;
(c) That ostensibly ordered variations in thickness are used to define the larger-scale LFS;
(d) That a new LFS begins when the thickness of a given HFS exceeds that of the underlying HFS.

The concept of a sedimentary hierarchy in ice-house platform carbonates as proposed by earlier workers can be formalized as the following definition:

> "a sedimentary hierarchy consists of two or more high-frequency sequences, each bounded by unambiguous evidence of sub-aerial exposure, in which there exists a repeated trend of

> decreasing high-frequency sequence thickness such that within a single low-frequency sequence each high-frequency sequence is thinner than the previous sequence ."

In this definition subaerial exposure surfaces define the thickness of an individual HFS. Stacking of these HFSs and trends of decreasing vertical thickness define any sedimentary hierarchy present.

In ice-house environments sub-aerial unconformities generally provide unambiguous evidence of a sea-level fall and can therefore be reasonably used as boundaries to HFSs. Greenhouse environments may also display evidence for sub-aerial exposure (e.g. Bover-Arnal *et al.* 2013, Cariou *et al.* 2013) although well-developed surfaces may be lacking (Haas, 2004), and so the selection of appropriate bounding surfaces is more difficult. For greenhouse carbonate successions, bounding surfaces could be reasonably placed at facies transitions that show an unequivocal fall of relative sea-level. An example of such a transition may be from inter-tidal to sub-tidal strata (Wright 1996). However, similar transitions can also occur due to autocyclic processes (Burgess 2001) and from tectonic-forcing overriding any eustatic controls (Bosence *et al.* 2009). A good understanding of three-dimensional stratal geometries and careful consideration of allo versus autocyclic processes (Burgess 2006) is therefore needed to define HFS boundaries in greenhouse strata. To avoid these issues, this study focuses on the definition of a HFS as it applies to ice-house cycles; i.e. bound by sub-aerial exposure surfaces.

Careful application of the above definition of hierarchy should decrease uncertainty in description and increase reproducibility from outcrop description. Further to this, numerical modelling can be used to give some indication as to the likelihood of creating hierarchical strata, as defined, under varying conditions arising from the combined interactions of eustatic controls of varying periodicity and amplitude. Absolute and even most relative age-dating of ancient successions is not able to differentiate individual HFSs at the scale of the interpreted cyclicity (<20-100ka), nor is it able to detect significant changes in sedimentation rate that may distort any original signal. Forward modeling therefore represents a method to determine how an ordered forcing mechanism is recorded as strata and allows us to examine the accuracy of the recording mechanism (Figure 2).

Model formulation

The model presented here is a one-dimensional numerical process-response stratigraphic forward model of carbonate accumulation (Pollitt 2008; Burgess and Pollitt, 2012). The model records accumulation on a simulated carbonate platform at a single point in space. Dominant processes affecting icehouse accommodation creation are glacio-eustatic sea-level change and subsidence (Burgess 2001; Barnett *et al.* 2002) which operate as independent variables. One-dimensional modelling lends itself well to the evaluation of stacking-patterns in platform top carbonates because aggradational stratal geometries are common in isolated platform interiors during ice-house periods (e.g. Goldhammer *et al.* 1994, Della Porta *et al.* 2002) and it is often assumed that high-frequency high-amplitude eustasy is a dominant control on stacking. Previous studies incorporating one-dimensional modelling of carbonate cyclicity have also attempted to address the conditions which would lead to Milankovitch-type 5:1 bundling of cycles (e.g. Walkden and Walkden, 1990). The benefit of using a simple one-dimensional model is that many thousands of long-duration simulations can be run allowing criteria such as thickness to be systematically evaluated against controlling parameters like eustatic period and amplitude, and production and subsidence rates.

Proponents of Milankovitch forcing of cyclic sequences have based their arguments primarily on the assumption that the periodicity of individual cycles (as calculated from numbers of cycles and sequence duration) commonly falls within the same range as that of Milankovitch-band parameters (20-400ka; Vail *et* al., 1977, Berger 1978). Intermediate-frequency oscillations, with periodicity of 100ka to 400ka, are commonly interpreted to oscillate with amplitude of 45-75m (Crowley and Baum 1991) although amplitudes of up to 95m have also been suggested (Heckel 1986, Read *et al*. 1986, Wright and Vanstone 2001). High-frequency oscillations are typically envisaged to have amplitudes up to 35m, with a periodicity of ~20ka to 40ka (e.g. Read *et al.* 1986, Paterson *et al.* 2006).

Allocyclic eustatic fluctuations forced by glacial build-up and melting are modelled using an asymmetrically-modified sinusoid, according to the function

$$f(x) = \begin{cases} \sin\left[\dfrac{\pi x}{\alpha}\right] \mathit{for} -\alpha/2 < x < \alpha/2 \ \mathit{and} \\ \sin\left[\dfrac{\pi}{2} + \dfrac{\pi}{\beta} \times \left(x - \alpha/2\right)\right] = \cos\left[\dfrac{\pi}{\beta} \times \left(x - \alpha/2\right)\right] \mathit{for}\ \alpha/2 < x \leq \alpha/2 + \beta \end{cases}$$

where α is the relative proportion of the period represented by the positive gradient limb, and β is the relative proportion of the period represented by the negative gradient limb. Outside this range $f(x)$ is defined to be periodic with period $\alpha + \beta$. Since this function is odd (i.e. $f(-x)= f(+x)$) its Fourier series consists of sines, therefore

$$f(x) = \sum b_n \times \sin\left[\frac{2\pi nx}{\alpha + \beta}\right]$$

where

$$b_n = \left[\frac{2}{\pi}\right] \times \left[\frac{1}{1+\frac{\beta}{\alpha}-2n} - \frac{1}{1+\frac{\beta}{\alpha}+2n} + \frac{1}{1+\frac{\alpha}{\beta}+2n} - \frac{1}{1+\frac{\alpha}{\beta}-2n}\right] \times \cos\left[\frac{\pi n}{1+\frac{\beta}{\alpha}}\right]$$

Carbonate accumulation

Carbonate accumulation is calculated iteratively according to operation of several simple processes summarised as

$$c_{(t)} = e_{(z)} + o_{(z)} + a_{(z)} \vee d_{(z)}$$

where *t* is time, *z* is platform surface elevation, and *c*, *e*, *o*, *a* and *d* are rates of carbonate accumulation, euphotic production, oligophotic production, aphotic production and surface lowering respectively. All rates are expressed in metres per million-years. Carbonate producers within the model are categorised as euphotic, oligophotic and aphotic (after Pomar 2001; Figure 3). Utilising multiple curves for carbonate production provides a way to define discrete lithofacies as simulation outputs, however this was not included in this study due to the aforementioned evidence against simple facies-depth relationships.

Euphotic biota are autotrophic and autoheterotrophic organisms requiring well-lit water and thus inhabiting shallow depths in the euphotic zone, which extends typically to 20-30m (Milliman 1974, Hallock and Schlager 1986). Estimates of euphotic zone sedimentation rates vary widely (e.g. Demicco and Hardie 2002; Strasser and Samankassou 2003) although they are well documented in modern environments for framework building organisms (e.g. Bosscher and Schlager 1993). The rates used in the model take into account the usually limited geographic extent of framework-building organisms in inner-platforms (*cf.* Smith and Kinsey 1976). The euphotic production component of the model is based on the work of Bosscher and Schlager (1993) and is applied in the model as

$$e_{(t)} = e_{(m)} \times \tanh\left[k \times \exp\left(d \times w_{(t)}\right)\right]$$

where w is water depth, t is the current timestep, e is carbonate accumulation, d is a decay constant and k is a rate constant.

Oligophotic organisms (autotrophic and autoheterotrophic) inhabit the oligophotic zone, characterised by lower light levels and sometimes lower temperature (Milliman 1974; Pomar 2001). Rates of production for deeper-water oligophotic carbonate factories are uncertain, but estimates suggest between 30-60% of euphotic factory rates (Pomar 2001; Schlager 2003). The oligophotic production component is represented by

$$o_{(t)} = o_{(m)} \times w_{(t)} < o_{(a)}$$
$$\Rightarrow \tanh\{o_{(k)} \times \exp[o_{(d)} \times (o_{(a)} - w_{(t)})]\} \vee \tanh\{o_{(a)} \times \exp[o_{(d)} \times (w_{(t)} - o_{(a)})]\}$$

where w is water depth, t is the current timestep, o is carbonate accumulation, a is a turn-around depth constant, d is a decay constant and k is a rate constant.

Production rates for aphotic sedimentation (from heterotrophic organisms) at shallow water depths are poorly constrained and are often categorised along with euphotic sedimentation rates (Pomar 2001). Aphotic sedimentation into deeper water is more constrained, with evidence from Pleistocene and Holocene data suggesting pelagic sedimentation to occur at a rate of 52-66m Ma^{-1} (Vollbrecht and Kudrass 1990). Aphotic production is modelled using the function

$$a_{(t)} = a_{(m)} \times w_{(t)} < a_{(w)} \Rightarrow w_{(t)} \times a_{(w)} \vee w_{(t)} < a_{(p)} \Rightarrow 1 - \left[\frac{(a_{(w)} - w_{(x)})}{(a_{(w)} - a_{(p)})}\right] \times a_{(r)} \vee a_{(r)}$$

where w is water depth, t is the current timestep, a is carbonate accumulation, p is a turn-around depth constant, r is a rate constant.

Model parameters and model runs

Each individual simulation in this study has a runtime of 3Ma. This was selected as an appropriately long duration to allow a significant number of LFSs to be generated. It also allows the simulated carbonate platform to come to a state of equilibrium relative to longer-term sea-level behaviour. A state of equilibrium in this model either means the platform always aggrades at or near sea-level or the platform drowns. Since the longest period of forcing simulated was 112ka, 3Ma allows for 26 such oscillations and therefore enough time to reach either state and determine if hierarchical strata form. Periodicities of oscillation were fixed at 23ka for high-frequency, 112ka for intermediate-frequency and 1Ma for low-frequency (Berger, 1978). Asymmetric sea-level oscillations are assumed to represent the faster melting of continental ice-sheets than their accumulation and typify ice-house sea-level behavior (de Boer and Smith 1994). High and intermediate-frequency oscillations were therefore modelled with 95% asymmetry while low-frequency oscillations were modelled as symmetrical (refer to Goldhammer 1991 for discussion of asymmetry in modelling sea-level behaviour). Although most of the other parameters and variables within the model are appropriate for both ice-house and greenhouse regimes, both the asymmetry and amplitude of the eustatic components are focused on characterizing the most likely sea-level behavior in ice-house periods.

Sensitivities to the iterative value (time-step) were evaluated by running a single simulation many times with different time-steps until a measured criterion became stable (i.e. did not vary between simulations). Through this sensitivity analysis a time-step of 0.000025Ma (25a) was selected. This time-step was chosen as it is at the upper limit of numerical stability (Figure 4).

Parameters varied in the simulations are given in Table 1. The range of sea-level amplitudes was chosen in order to bracket the range of oscillation amplitudes documented in published literature (e.g. Heckel 1986; Crowley and Baum 1991; Wright and Vanstone 2001). Subsidence was modelled at a constant rate, varied within a range considered to represent a reasonable spectrum of likely scenarios. A minimum rate of 10m Ma^{-1} was modelled in order to represent intra-cratonic basins while a maximum rate of 900m Ma^{-1} was considered to represent a rapidly subsiding basin on an active plate margin.

The simulations presented in this study did not include any sub-aerial denudation during exposure since rates of carbonate dissolution from ancient platforms are poorly constrained. Although some empirical estimates of carbonate dissolution are available (e.g. Plan, 2005) the high degree of uncertainty surrounding these values as applied to ancient platform interior sediments introduces significant complexity into evaluating the response of stratigraphy to external forcing. Additionally, including erosion makes comparison with previous studies that did not invoke erosion (e.g. Goldhammer *et al*. 1994) more troublesome. Future work will be needed to quantify the effect of sub-aerial denudation on the likelihood of generating a sedimentary hierarchy.

In each simulation a parameter is modified within the range according to a predefined stepping value, thus each simulation represents the unique combination of the five variables. 110,000 simulations were run, spanning the complete range of all five variables.

Model Output

Although the model outputs simulated thickness and chronostratigraphic sections (Figure 2) that are visually similar to outcrop measured sections a more quantitative measure of hierarchy is required to objectively compare both simulated and outcrop examples. This measure is used to provide a single value per simulation that could be evaluated statistically across several thousand model runs.

This metric is presented here as a ratio which represents the number of HFSs per LFS and is referred to as the "*h*-value". The calculation of *h* is made with complete information in both a time and thickness-domain since within the model all parameters and responses are known. The *h*-value can be expressed as $1/n$, where *n* is the number of HFSs (Figure 5). This provides a convenient way of comparing the degree of hierarchy development from multiple simulations. In a strongly non-hierarchical system, for instance, there may only be one HFS per LFS, which would result in a ratio of 1:1 (or h=1). Over the course of a 3Ma simulation there will be occasions when more than one HFS occurs per LFS, and so the average ratio for the entire simulation would be $h<1$. If conditions consistently allowed two HFSs per LFS, the ratio would be h=0.5, and if there were three then h=0.33. By this measurement and the definition of hierarchy employed here, a sedimentary section, simulated or otherwise, can be considered to display weak evidence of a sedimentary hierarchy if there are on average >=2 HFSs per LFS ($h<0.5$), and strong evidence of a sedimentary hierarchy if there are on average >=3HFSs per LFS ($h<0.33$).

Results

Figure 6 shows the results of four simulations where the amplitude of the high-frequency eustatic component has been varied to result in *h*-values reflecting a range of hierarchical and non-hierarchical outcomes. All parameters except high-frequency amplitude were constant in these simulations, including intermediate-frequency amplitude which was fixed at 40m. As high-frequency amplitude increases, more oscillations of sea-level are recorded as discrete units of sedimentation separated by sub-aerial exposure surfaces (i.e. a HFS). This is a direct consequence of amplitude, since higher amplitude oscillations have a greater likelihood of exposing the platform.

Figure 7 displays the corresponding stratigraphic diagrams to the chronostratigraphic results shown in Figure 6. All simulations produce stratigraphic sections that resemble metre-scale ice-house HFSs described from outcrop. Variation in the amplitude of high-frequency oscillation results in markedly different cycle thicknesses although all simulations generate a similar total sediment thickness (204-219m). Non-hierarchical sections (h>0.5) have cycle thicknesses that are roughly similar to those described from outcrops of ice-house platform carbonates (10-15m). Weakly to strongly hierarchical sections (h<0.5) display thinner cycles the higher the h-value. The most hierarchical section has an average cycle thickness of 6.06m. This is thinner than usually described from ice-house successions and is a consequence of having rapid glacio-eustatic oscillations; many oscillations are recorded as discrete periods of sedimentation, but since the oscillations are of short-duration the resulting cycles are thin.

The likelihood of generating a sedimentary hierarchy for 110,000 parameter combinations across the investigated range is shown in Figure 8. These results are displayed in the chronostratigraphic time-domain and show that only 9% of possible parameter values lead to strata displaying at least weak evidence of a sedimentary hierarchy (i.e. having on average two HFSs per LFS or $h<0.5$). Furthermore, only 4% of simulations display strong evidence of a sedimentary hierarchy (having on average three HFSs per LFS or $h<0.33$).

The cumulative probability distribution for these results shows that the majority of simulations (78%) have $h>0.75$ meaning that these simulations average between 1 and 2 HFSs per LFS (Figure 8). These 78% of models run do not exhibit consistent trends of vertically decreasing thickness within a LFS and so do not generate hierarchical strata. This suggests that hierarchies are created only under a specific and limited set of allocyclic forcing conditions.

The cumulative probability distribution for the same set of simulations but for a thickness-domain hierarchy shows that based on analysis of thickness alone (Figure 9), without additional information about, for example, duration of deposition, only 15% of simulations exhibit weak evidence of a sedimentary hierarchy. Furthermore less than 1% of simulations display strong evidence of a sedimentary hierarchy. In contrast to results measured in the chronostratigraphic time-domain, where a majority of simulations showed strong evidence against a sedimentary hierarchy ($h>0.75$), thickness-domain results show relatively few simulations with either very strong evidence for or against a hierarchy. Fewer than 1% display strong evidence for a hierarchy ($h<0.33$) and only 6% display strong evidence against a hierarchy ($h>0.75$). The majority of simulations therefore have between 1.5 and 2 HFSs per LFS demonstrating that when measured in the thickness-domain alone, most modelled strata display evidence against a sedimentary hierarchy.

Using the parameter-space distribution of time-domain hierarchical and non-hierarchical simulations we can investigate further why evidence for a thickness hierarchy is weaker than combined time-thickness evidence (Figure 10). Under relatively simple conditions with only two eustatic variables there is a clear relationship between amplitude of low-frequency oscillation relative to that of intermediate-frequency oscillation and the ability to generate a hierarchy. It is only when the amplitude of high-frequency oscillation exceeds ~70% of the intermediate-frequency amplitude that hierarchies are consistently generated throughout a simulated section (i.e. returning an average of h<0.5). This relationship between relative amplitudes of oscillation also provides an insight into why simulations with the most extreme h-values occur. The least hierarchical strata occur when intermediate-frequency amplitude is greatest, while the most strongly hierarchical strata form when high-frequency amplitude is largest and so end-member h-values are limited to extremes of oscillation amplitude.

The distribution of h-values for this group of simulations is without discrete steps or tipping points (Figure 11). As the relative amplitude of high- to intermediate-frequency oscillations increases, the mean h-value of the simulated strata also increases. For the range of parameter values tested here, a hierarchy is increasingly likely with increasing higher-frequency eustatic oscillation relative to the amplitude of the lower frequency oscillation. Given these results, if the amplitude of high-frequency eustatic oscillations is known for given strata (in the Pleistocene for instance), it may be possible to estimate the h-value range and likely intermediate-frequency amplitude.

Examination of a single hierarchical and a single non-hierarchical example from this parameter-space distribution provides insight into why this relationship exists (Figure 12). In the non-hierarchical case fourteen HFSs are generated. Nine HFSs are clearly forced by the intermediate-frequency sea-level oscillation and five HFSs are forced by a high-frequency oscillation of sea-level during the falling-stage of an intermediate-order oscillation. The small amplitude high-frequency oscillation (20m) during the relatively large amplitude intermediate-frequency oscillation (90m) provides only a short interval during the falling-stage of the intermediate-frequency oscillation when a HFS can be generated. In contrast, in the hierarchical example during the same period, 33 HFSs are created because the high-frequency higher-amplitude oscillations have a much greater impact on the geometry of the relative sea-level curve. Instead of only triggering deposition during the falling stage of an intermediate-frequency oscillation, higher amplitude high-frequency oscillations are sufficient to regularly trigger and then truncate sedimentation regardless of the position on the intermediate-frequency curve. This creates hierarchical strata with many HFSs per LFS.

Stratigraphic completeness in these two simple examples is surprisingly similar given the variation in regularity of exposure events (Figure 12). In both cases, mean stratigraphic completeness is calculated by determining the percentage of time during each HFS where sedimentation occurs. The mean value represents the average for all HFSs over the entire simulation. These results do not suggest that hierarchical strata will tend to be more incomplete than non-hierarchical strata. In this example, the non-hierarchical example has average stratigraphic completeness of 49%, while the hierarchical example is 47% complete. In both of these cases the minimum and maximum values for stratigraphic completeness are similar, suggesting that in each simulation there are end-members of similarly long and short periods of sedimentation. Although short duration sub-aerial exposure occurs more regularly in the hierarchical simulation, the non-hierarchical simulation has long periods of less frequent exposure at intermediate-frequency lowstands of sea-level. The net result is similar overall periods of non-deposition.

Although the relationship between hierarchy and stratigraphic completeness is straightforward under these simple forcing conditions, as the complexity of multiple nested eustatic curves is introduced the incidence of hierarchical strata decreases. This is demonstrated in Figure 13 with the addition of a third forcing component; a eustatic curve with a 1Ma symmetric oscillation of varying amplitude. Generally, as the amplitude of this eustatic component increases, fewer cases of hierarchical strata occur. More rapid accommodation change results in a greater likelihood of drowning during the transgressive stage.

Burgess and Pollitt (2012) used the same forward model to study controls on lithofacies thickness distributions. They showed that increasing the complexity of the forcing eustatic curve with additional frequencies of oscillation created exponential thickness distributions of the kind observed in outcrop. Simpler curves created non-exponential thickness distributions. Exponential thickness distributions are significant because statistical theory suggests that they arise from random processes. Burgess and Pollitt (2012) showed that they can also arise from complex forcing functions in a deterministic model when rapid changes in water depth generate strata with many thin lithofacies units and few thick lithofacies units. Aside from raising interesting issues about the nature of randomness versus complexity, this result is significant here because more complex forcing also tends to decrease the likelihood of hierarchical strata. These results suggest that hierarchical strata represent the effects of simple external forcing and not complex interactions of multiple forcing components, as previous workers have suggested (e.g. Paterson *et al.* 2006).

Only 9% of the 10,000 simulations shown in Figure 13 show at least weak evidence for a time-domain hierarchy and these are restricted to a relatively small region of parameter-space. This small region represents a 'Goldilocks' zone of suitable parameters for time-domain hierarchy development. In the case of the model runs represented by Figure 13 this zone represents the following conditions:

1. Subsidence rate is sufficient for development of stacked cycles rather than a continuously exposed platform (>=100m Ma^{-1}).
2. Subsidence rate is not so high that accommodation significantly outpaces sediment supply and drowns the carbonate factory (<500m Ma^{-1}).
3. The low-frequency forcing component is of low amplitude (<120m). Higher amplitudes increase the likelihood of drowning and decrease the potential for generation of hierarchical strata.
4. The high-frequency forcing component is of sufficient amplitude to regularly cause HFS development (>70% that of intermediate-frequency amplitude).

These criteria are true for this particular rate of maximum carbonate productivity (2000m Ma^{-1}). Different productivity rates would change the zone of preferential hierarchy development. These results support the view that hierarchical strata require quite specific conditions to develop and so are likely to be relatively rare.

The results depicted in Figure 13 demonstrate the range of modelled parameter values in which hierarchies defined in the chronostratigraphic domain can occur. Figure 14 shows thickness-domain (stratigraphic) results from the same set of simulations with *h*-value calculated from thickness information alone. Stratigraphic hierarchies observed in model results may be used to infer how likely it is that a hierarchy can be reasonably interpreted from outcrop. In these cases, the *h*-value represents the degree of hierarchy development indicated by stacking of HFS thickness, where a new LFS is started if a given HFS is thicker than the last. Figure 14 shows that using a thickness-only definition there is a broader parameter-space range in which hierarchical sections may be identified. However, fewer model runs can be categorized as strongly hierarchical. There is less of a dependency on low-frequency amplitude, with apparently hierarchical sections occurring at large low-frequency amplitudes. Similarly, high *h*-values are recorded at low subsidence rates, although drowning of the platform still terminates hierarchy development above rates of 400 m Ma^{-1}.

These two different methods of defining hierarchies give different results because many examples of hierarchies defined using thickness information do not constitute hierarchies when considered using full chronostratigraphic information (e.g. Figure 2). Indications of hierarchy from thickness data alone are often inaccurate. This effect is particularly acute if high-frequency oscillations are of large amplitude. In these cases high-frequency oscillations regularly force HFS deposition on the transgressive part of the intermediate-frequency curve. Although of short-duration, these HFSs are often thicker than the underlying HFS and would be identified, using thickness information alone, as a new LFS. An example of this behavior is shown in Figure 2. When analysed using thickness information alone, these strata appear hierarchical when in a true sense they are not. A significant number of the hierarchical sections shown in Figure 14 can be considered false-positives. In these situations the hierarchy present in the stacking patterns of HFS thickness is not truly representative of the forcing mechanism since the LFSs in these sections will be composed of HFSs forced by different oscillations of sea-level (as is the case in Figure 2). In effect, HFSs are bundled incorrectly and the stratigraphic record – in the process of converting a time-domain sedimentation rate to the thickness-domain – is an imperfect record. This result suggests that determining which sections truly display stacking representative of the forcing mechanism is not possible using thickness information alone. Comparison between the number of strongly-hierarchical simulations in the time-domain versus the much greater number of weakly-hierarchical simulations in the thickness-domain suggests that the wide distribution of hierarchical sections indicated by the thickness-only analysis is not an accurate representation of the forcing mechanism and over-estimates the number of hierarchical simulations.

Comparison to outcrops

Results from the model runs discussed above suggest that truly hierarchical strata are relatively rare and restricted to a small area of the modelled parameter-space. However, hierarchies defined based on thickness data have been defined many times, both explicitly and implicitly, in the interpretation of carbonate outcrops. Lehrmann and Goldhammer (1999) contained interpretations of data from 93 outcrops, five of which contained explicit interpretations of sedimentary hierarchies composed of stacked "4th-order parasequences" (LFSs) and "5th-order parasequences" (HFSs) and based on thickness trends. For instance, the Hermosa Group logged by Goldhammer *et* *al.* (1994) is defined as "composite stratigraphic cyclicity, in which small depositional cycles build into larger sequences according to vertical stacking patterns" (Goldhammer *et al.* 1994; p267) and is clearly defined by diagrams in that study. Two of these five outcrops, the Pennsylvanian Hermosa Group and Gobbler Formation in the south-western USA were also logged independently by Pollitt (2008; Figure 15). Figure 16 shows the hierarchy *h*-value as per the original workers' interpretation of HFSs and LFSs as well as the *h*-value using the HFS definition made in this study.

h-values resulting from the original worker's interpretation of HFSs and LFSs range from 0.08 to 0.30. This is aligned with the interpretation that these sections are hierarchical (e.g. Goldhammer *et al.* 1994). However using the hierarchy definition made in this study (i.e. consistently starting a new LFS when a given HFS is thicker than the last) results in higher *h*-values ranging from 0.57 to 0.75, suggesting that in fact the strata are not hierarchical in any meaningful sense. In these cases a rigorous application of stacking according to vertical thickness does not result in a hierarchy, but instead results in approximately 1.6 HFSs per LFS which is not representative of Milankovitch bundling ratios. Similarly, the Holder and Gobbler Formations, described as cyclic by previous workers (Wilson 1972; Algeo *et al.* 1991), respectively have *h*-values of 0.65 and 0.76 which equates to an average of 1.5 and 1.3 HFSs per LFS.

The fact that all seven cases shown in Figure 16 were interpreted as hierarchical based on thickness and stacking patterns but this was not reproduced with a more rigorous definition suggests that workers have an inherent bias towards inferring patterns of order in sedimentary sections.

Analysis of the remaining 88 sections in the data published by Lehrmann and Goldhammer (1999) suggests that *h*-values are relatively consistent and usually within the range h=0.6-0.7 (Figure 17). This is surprising given that the data comes from a wide variety of depositional settings and ages from the Paleozoic to Cenozoic. The outlying datapoints (Figure 17) are likely to be a result of undersampling in terms of number of HFSs. Sequences with less than 20 HFSs show greater scatter than those with n>20 (Figure 18). This data suggests that in the majority of these measured sections, when a rigorous definition of a sedimentary hierarchy is applied, the number of HFSs per LFS is between 1.5 and 2. This is not suggestive of any type of bundling according to climatic forcing, and suggests that consistent vertical trends in HFS thickness are not present in any of the studied outcrops. Analysis of the number of "runs" of decreasing or increasing lithofacies unit thickness in the Lehrmann and Goldhammer (1999) dataset shows that there are typically approximately two lithofacies units in a given run (Figure 19). This data suggests that long term consistent trends in lithofacies unit thickness are rare and most are indistinguishable from random, a finding which supports that of earlier workers (Wilkinson *et al.* 1996). It also suggests the possibly of bias inherent to stratigraphic interpretation, where workers tend to 'even out' thickness of lithofacies units and avoid extremes in thickness (Burgess 2008); where thin units are rarely interpreted and are commonly lumped as interbeds and thick units are broken into smaller units using a variety of criteria such as sorting or grainsize.

Discussion

"All models are wrong, but some are useful" (Box 1987) is an important statement to consider when interpreting the results from any type of forward model. The one-dimensional forward modelling in this study, while certainly simplistic and "wrong" in many respects, is useful in the sense that it forces us to objectify and quantify our concept and definition of sedimentary hierarchies in carbonate successions. Key assumptions in the model have a strong bearing on its output. In the case of generating a sedimentary hierarchy, key assumptions are the parameters relating to the ordered forcing of sea-level behavior and the definition of a sedimentary hierarchy.

Clearly the results presented here are very dependent on the definition of hierarchy. Different results would be obtained with a different definition. Other definitions of a hierarchy are certainly possible and have been employed elsewhere. For instance, a hierarchy could be defined in terms of facies partitioning whereby proportions of facies are altered relative to depositional position within a systems tract. This may be particularly important in greenhouse environments and to evaluate hierarchies in greenhouse strata it is likely that further model runs are required with greenhouse-specific parameters (e.g. low-amplitude oscillations, autocyclic component). A comparison of the occurrence of hierarchies by different definitions in a controlled model environment could be important future work.

With these limitations in mind, these results from numerical modelling suggest that forcing by ordered cyclical sea-level oscillations rarely results in an easily identifiable hierarchy of stacked cycles, defined either with total chronostratigraphic information (9% of cases) or with just thickness data (15% of cases). The fact that only 9% of sections result in a hierarchical chronostratigraphic section is particularly illuminating, since it suggests that vertically decreasing trends in thickness are not an appropriate way to identify ordered patterns in sea-level behavior. Were this not true, then clearer trends in duration of HFS deposition would result from the trends in accommodation caused by oscillation of sea-level (as depicted conceptually in Figure 1).

One key difference between the conceptual depiction in Figure 1 and the model simulations conducted in this study is the periodicity of orbital oscillation. In the conceptual example, and in many other numerical studies of nested cyclicity (e.g. Goldhammer 1994) the period of the high-frequency oscillation is evenly divisible from the intermediate-frequency, such that five high-frequency cycles fit exactly within one intermediate-frequency oscillation. High-frequency cycles therefore occur in the exact same position relative to the intermediate-frequency oscillation on a consistent basis. There is no reason to expect Milankovitch parameters to be evenly divisible in this way. Behavior of individual Milankovitch-scale orbital variations is known to vary through time quasi-chaotically, suggesting that such a state is unlikely to occur and be maintained over a significant period (Laskar *et al.* 2011). Given this, it seems more reasonable in this simple model to simulate sedimentation with periodicities that vary relative to one another through time, meaning that high-frequency oscillations occur in different relative positions to each intermediate-frequency oscillation (for an example see Figure 6).

The net effect of variation in the relative position of high-frequency oscillations is to change the duration and thickness of HFSs in each successive intermediate-frequency oscillation. Thus the hierarchy depicted in Figure 1 cannot occur, and this has a fundamental effect on generation of the vertical thickness trends used to identify hierarchies. For example, it means that the thickest HFS is not always at the start of an intermediate-frequency oscillation and the thinnest HFS is not always at the end. This leads to thickness trends that do not always bear an obvious relationship to the sequence stratigraphic position and vary significantly from the simple and convenient conceptual models put forward by earlier workers. It also means that vertical trends in cycle thickness alone should not be used to identify hierarchies of stratigraphic cyclicity. Given this, are existing qualitative models of carbonate sequence stratigraphy useful? Where the nature of bundling of higher-frequency sequences in lower-frequency sequences changes through time, it is probably not possible to describe cycle stacking with a single simple conceptual model. Given these important implications, further research into the ability to generate sedimentary hierarchies under different combined periodicities of orbital oscillation may increase our understanding of where hierarchies are likely to occur.

Results presented here demonstrate that even in a simple 1D model, strata may not accurately represent the signal from external forcing factors. For example, in Figure 2, the LFSs defined in the thickness domain do not correspond to those defined in the time-domain. In this case, thickness of successive HFSs, although decreasing vertically, span multiple oscillations of intermediate-frequency eustatic sea-level and so cannot be said to accurately record the forcing mechanism. In this sense, even a much-simplified representation of the stratigraphic record is demonstrated to be an imperfect record of hierarchies on the basis of vertical thickness trends. Comparison of model results to outcrop data supports this conclusion and suggests that even for the best documented examples of hierarchies in carbonate strata the degree of vertical trends in cycle stacking is likely to be overstated when a strict definition of a hierarchy is applied.

In these model results, hierarchies occur in only a small region of parameter space. This raises the question what happens in the remaining >80% of the parameter space where hierarchies do not occur? Are there other stratal patterns that reflect order arising from allocyclic forcing that have not yet been described? It is also interesting to consider how introduction of additional complexity such as sediment erosion, transport and diagenesis in 3D would affect occurrence of hierarchical strata. Could some parts of a carbonate platform preserve a stratal hierarchy while others do not? Further experimental work combined with careful outcrop examination is required to investigate all of these questions.

Conclusions

1. The numerical forward modeling experiments presented here investigate the response of depositional systems if they were to behave in the way implied by sequence stratigraphic (hierarchical) models. This model is internally-consistent and uses plausible parameters.
2. These experiments suggest that in the simplest cases, with two superimposed orders of allocyclic forcing, the higher-frequency forcing needs to have an amplitude of 70% that of the lower-frequency oscillation in order to consistently effect cyclicity and generate a sedimentary hierarchy. Additional frequencies of allocyclic forcing attenuate the eustatic curve further and decrease the likelihood of any hierarchy being preserved in the stratigraphic record.
3. Results from a wide range of allocyclic forcing amplitude, subsidence and carbonate production rates suggest that ordered forcing via cyclical eustatic sea-level change rarely results in an easily identifiable hierarchy of stacked cycles. Hierarchies defined with full chronostratigraphic information occur in 9% of model run cases, and in 15% of cases when defined purely in terms of thickness information.

4. The lack of a significant number of strongly and weakly hierarchical sections suggests vertical thickness trends in strata are unlikely to be hierarchical, even in situations where external forcing is present.
5. Hierarchical sections do not intrinsically contain more missing time than non-hierarchical sections. Hierarchical sections necessarily miss fewer “beats” than non-hierarchical sections, but simulations from the two groups can show a similar amount of missing time; non-hierarchical sections can be just as incomplete as hierarchical sections.
6. Strata that appear weakly hierarchical in the thickness-domain are unlikely to be representative of the true ‘bundling’ of orbital forcing parameters. If frequencies of oscillation vary through time, relative to one another, the resultant variability in attenuation of the relative sea-level curve results in significant variation in sediment thickness per oscillation. This has a tendency to disrupt trends of vertical thickness and leads to false-positive identification of hierarchical sections. This also suggests that vertical thickness trends are not an appropriate proxy for identify eustatic forcing events in shallow-water carbonate platforms.
7. Comparison to studied outcrops suggests that hierarchies defined in terms of stratigraphic thickness are often assumed to be present despite a lack of adequate supporting evidence. Quantitative analysis of many of these sections suggests that they are not in fact hierarchical in any meaningful sense.

Acknowledgements

The authors are grateful to Dan Lehrmann for providing the data published in Lehrmann and Goldhammer (1999). Thanks also to Dan Bosence and Bruce Wilkinson for their thorough critique of the original manuscript which prompted numerous and significant revisions.

References

ALGEO, T. J. AND HINNOV, L. A. 2006. Milankovitch cyclicity in the Ohio and Sunbury shales: astronomical calibration of the Late Devonian-Early Carboniferous Timescale (Abstract). *Geological Society of America Abstracts with Programs,* **38,** 268.

Algeo, T. J., Wilson, J. L. and Lohmann, K. C. 1991. Eustatic and tectonic controls on cyclic sediment accumulation patterns in Lower-Middle Pennsylvanian strata of the Orogrande Basin, New Mexico. In *Geology of the Sierra Blanca, Sacramento and Capitan Ranges, New Mexico: New Mexico Geological Society Guidebook. 42nd Field Conference*, (ed. Barker, J. M., Kues, B. S., Austin, G. S. and Lucas, S. G.), New Mexico Geological Society, 1991 Field Conference, 203-12.

Barnett, A.J., Burgess, P.M. and Wright, V.P. 2002. Icehouse world sea-level behaviour and stratal patterns in late Visean (Mississippian) carbonate platforms; integration of numerical forward modelling and outcrop studies. *Basin Research*, **14,** 417-439.

Barrell, J. 1917. Rhythms and the Measurements of Geologic Time: Bulletin of the Geological Society of America, **28**, 745-904.

Berger, A. L. 1978. Long-term variations of caloric insolation resulting from the Earth's orbital elements. *Quaternary Research,* **9,** 139-67.

Bosence, D., Procter, E., Aurell, M., Bel Kahla, A., BouDagher-Fadel, M. K., Casaglia, F., Cirilli, S., Mehdie, M., Nieto, L., Rey, J., Scherreiks, R., Soussi, M. and Waltham., D. 2009. A dominant tectonic signal in high-frequency, peritidal carbonate cycles? A regional analysis of Liassic platforms from western Tethys. *Journal of Sedimentary Research*, **79**, 389-415.

Bosscher, H. and Schlager, W. 1993. Accumulation rates of carbonate platforms. *Journal of Geology*, **101,** 345-355.

Bover-Arnal, T. and Strasser, A. 2013. Relative sea-level change, climate, and sequence boundaries: insights from the Kimmeridgian to Berriasian platform carbonates of Mount Salève (E France*), International Journal of Earth Sciences*, **102**, 493-515.

Box, G.E.P. and Draper, N.R. 1987. *Empirical Model-Building and Response Surfaces*. Wiley, New York, 424 pp.

Budd, D. A., Gaswirth, S. B. and Oliver, W. L. 2002. Quantification of macroscopic subaerial exposure features in carbonate rocks. *Journal of Sedimentary Research,* **72,** 917-28.

Burgess, P. M. 2001. Modelling carbonate sequence development without relative sea-level oscillations. *Geology,* **29,** 1127-30.

Burgess, P. M. 2006. The signal and the noise: forward modeling of allocyclic and autocyclic processes influencing peritidal carbonate stacking patterns. *Journal of Sedimentary Research,* **76,** 962-77.

Burgess, P.M. 2008. The nature of shallow-water carbonate lithofacies thickness distributions. *Geology*, **36,** 235-238.

Burgess P. M. and Pollitt, D. A. 2012. The origins of shallow-water carbonate lithofacies thickness distributions: one-dimensional forward modelling of relative sea-level and production rate control. *Sedimentology*, **59**, 57–80.

Cariou, E., Olivier, N., Pittet, B., Mazin, J.-M. and Hantzpergue, P. 2013. Dinosaur track record on a shallow carbonate-dominated ramp (Loulle section, Late Jurassic, French Jura), Facies, *In Press*.

Cozzi, A., Hinnov, L. A. and Hardie, L. A. 2005. Orbitally forced Lofer cycles in the Dachstein Limestone of the Julian Alps (northeastern Italy). *Geology,* **33,** 789-92.

Crowley, T.J. and Baum, S.K. 1991. Estimating Carboniferous sea-level fluctuations from Gondwanan ice-extent. *Geology*, **19,** 975-977.

Davies, J. R. 1991. Karstification and pedogenesis on a late Dinantian carbonate platform, Anglesey, North Wales. *Proceedings of the Yorkshire Geological Society,* **48,** 297-321.

de Boer, P.L. and Smith, D.G. 1994. Orbital forcing and cyclic sequences. In: *Orbital Forcing and Cyclic Sequences* (Eds P.L. de Boer and D.G. Smith), *IAS Special Publication*, **19**, pp. 1-14. IAS, Oxford.

Della Porta, G., Kenter, J. A. M., Immenhauser, A. and Bahamonde, J. R. 2002. Lithofacies character and architecture across a Pennsylvanian inner-platform transect (Sierra de Cuera, Asturias, Spain). *Journal of Sedimentary Research,* **72,** 898-916.

Demicco, R. V. and Hardie, L. A. 2002. The "carbonate factory" revisited: a re-examination of sediment production functions used to model deposition on carbonate platforms. *Journal of Sedimentary Research,* **72,** 849-57.

Drummond, C. N. and Wilkinson, B. H. 1993a. Carbonate cycle stacking patterns and hierarchies of orbitally forced eustatic sea-level change. *Journal of Sedimentary Petrology,* **63,** 369-77.

Drummond, C. N. and Wilkinson, B. H. 1993b. On the Use of Cycle Thickness Diagrams as Records of Long-Term Sealevel Change during Accumulation of Carbonate Sequences. *The Journal of Geology,* **101,** 687-702.

Drummond, C. N. and Wilkinson, B. H. 1996. Stratal thickness frequencies of and the prevalence of orderedness in stratigraphic sequences. *Journal of Geology,* **104,** 1-18.

Goldhammer, R. K., Dunn, P. A. and Hardie, L. A. 1987. High frequency glacio-eustatic sealevel oscillations with Milankovitch characteristics recorded in Middle Triassic platform carbonates in northern Italy. *American Journal of Science,* **287,** 853-92.

GOLDHAMMER, R. K., DUNN, P. A. AND HARDIE, L. A. 1990. Depositional cycles, composite sea level changes, cycle stacking patterns, and the hierarchy of stratigraphic forcing: example from platform carbonates of the Alpine Triassic. *Geological Society of America Bulletin,* **102,** 535-62.

GOLDHAMMER, R.K., OSWALD, E.J. AND DUNN, P.A. 1991. Hierarchy of stratigraphic forcing: example from Middle Pennsylvanian shelf carbonates of the Paradox Basin. In: *Sedimentary Modeling: Computer Simulations and Methods for Improved Parameter Definition* (Eds E.K. Franseen, W.L. Watney, C.G.S.C. Kendall and W. Ross), *Kansas Geological Survey Bulletin*, **233**, 361-414. Kansas Geological Survey, Lawrence, KS.

GOLDHAMMER, R. K., OSWALD, E. J. AND DUNN, P. A. 1994. High-frequency, glacio-eustatic cyclicity in the Middle Pennsylvanian of the Paradox Basin: an evaluation of Milankovitch forcing. In *Orbital Forcing and Cyclic Sequences*, (ed. DE BOER, P. L. AND SMITH, D. G.), **19**. IAS Special Publication, Oxford, 243-83.

HAAS, J. 2004. Characteristics of peritidal facies and evidences for subaerial exposures in Dachstein-type cyclic platform carbonates in the Transdanubian Range, Hungary. *Facies,* **50,** 263-86.

HALLOCK, P. AND SCHLAGER, W. 1986. Nutrient excess and the demise of coral reefs and carbonate platforms. *Palaios*, **1,** 389-398.

HECKEL, P.H. 1986. Sea-level curve for Pennsylvanian eustatic marine transgressive-regressive depositional cycles along midcontinent outcrop belt, North America. *Geology*, **14,** 330-334.

KERANS, C., LUCIA, F. J. AND SENGER, R. K. 1994. Integrated characterization of carbonate ramp reservoirs using Permian San Andres Formation outcrop analogs. *American Association of Petroleum Geologists Bulletin,* **78,** 181-216.

Kenter, J. A. M., Harris, P. M., Collins, J. F., Weber, L. J., Kuanysheva, G. and Fischer D. J., 2006. Late Visean to Bashkirian Platform Cyclicity in the Central Tengiz Buildup, Precaspian Basin, Kazakhstan: Depositional Evolution and Reservoir Development. In *Giant Hydrocarbon Reservoirs of the World: From Rocks to Reservoir Characterization and Modeling*, (ed. Harris, P. M. and Weber, L. J.), AAPG Memoir, **88**, 55-95.

LASKAR, J., FIENGA, A., GASTINEAU, M. AND MANCHE, H. 2011. La2010: a new orbital solution for the long-term motion of the Earth. *Astronomy and Astrophysics*, **532**, A89

LEHRMANN, D. J. AND GOLDHAMMER, R. K. 1999. Secular variation in parasequence and facies stacking patterns of platform carbonates: a guide to application of stacking patterns analysis in strata of diverse ages and settings. In *Advances in Carbonate Sequence Stratigraphy: Applications to Reservoirs, Outcrops and Models*, (ed. SALLER, A. H., HARRIS, P. M. AND SIMO, J. A.), SEPM Special Publication, **63**. SEPM, Tulsa, Oklahoma, 187-225.

LERAT, O., VAN BUCHEM, F. S. P., ESCHARD, R., GRAMMER, G. M. AND HOMEWOOD, P. W. 2000. Facies distribution and control by accommodation within high-frequency cycles of the Upper Ismay interval (Pennsylvanian, Paradox

Basin, Utah). In *Genetic Stratigraphy at the Exploration and Production Scales*, (ed. Homewood, P. W. and Eberli, G. P.), Elf EP, Pau, France, 71-91.

Milliman, J. D. 1974. *Marine Carbonates. Part 1, Recent Sedimentary Carbonates*. Springer-Verlag, New York, 375 pp.

Paterson, R. J., Whitaker, F. F., Jones, G. D., Smart, P. L., Waltham, D. A. and Felce, G. 2006. Accommodation and sedimentary architecture of isolated icehouse carbonate platforms: insights from forward modeling with CARB3D+. *Journal of Sedimentary Research,* **76,** 1162-82.

Plan, L., 2005. Factors controlling carbonate dissolution rates quantified in a field test in the Austrian alps. *Geomorphology*, **68**, 201-12.

Pollitt, D.A. 2008. *Outcrop and forward modelling analysis of ice-house cyclicity and reservoir lithologies*. PhD thesis, Cardiff University, UK.

Pomar, L. 2001. Types of carbonate platforms: a genetic approach. *Basin Research,* **13,** 313-34.

Rankey, E. C. 2004. On the Interpretation of Shallow Shelf Carbonate Facies and Habitats: How Much Does Water Depth Matter? *Journal of Sedimentary Research,* **74,** 2-6.

Read, J. F., Grotzinger, J. P., Bova, J. A. and Koerschner, W. F. 1986. Models for generation of carbonate cycles. *Geology*, **14**, 107-10.

Saller, A. H., Dickson, J. A. D. and Boyd, S. A. 1994. Cycle stratigraphy and porosity in Pennsylvanian and Lower Permian shelf limestone, Eastern Central Basin Platform, Texas. *American Association of Petroleum Geologists Bulletin,* **83,** 1835-54.

Sattler, U., Immenhauser, A., Hillgärtner, H. and Esteban, M. 2005. Characterization, lateral variability and lateral extent of discontinuity surfaces on a Carbonate Platform (Barremian to Lower Aptian, Oman). *Sedimentology,* **52,** 339-61.

Schlager, W. 2003. Benthic carbonate factories of the Phanerozoic. *International Journal of Earth Sciences,* **92,** 445-64.

Schwarzacher, W. 2005. The stratification and cyclicity of the Dachstein Limestone in Lofer, Leogang and Steinernes Meer (Northern Calcareous Alps, Austria). *Sedimentary Geology,* **181,** 93-106.

Smith, S. V. and Kinsey, D. W. 1976. Calcium carbonate budget production, coral reef growth and sea-level changes. *Science,* **194,** 937-39.

Strasser, A. and Samankassou, E. 2003. Carbonate Sedimentation Rates Today and in the Past: Holocene of Florida Bay, Bahamas, and Bermuda vs. Upper Jurassic and Lower Cretaceous of the Jura Mountains (Switzerland and France). *Geologia Croatica,* **56,** 1-18.

Vail, P. R., Mitchum, R. M. J., Todd, R. G., Widmier, J. M., Thompson, S. I., Sangree, J. B., Bubb, J. N. and Hatlelid, W. G. 1977. Seismic stratigraphy and global changes of sea level. In *Seismic Stratigraphy: Applications to Hydrocarbon Exploration*, (ed. Payton, C. E.), AAPG Memoir, **26**. AAPG, Houston, 49-212.

Vanstone, S. D. 1998. Late Dinantian palaeokarst of England and Wales: implications for exposure surface development. *Sedimentology,* **45,** 19-37.

Vollbrecht, R. and Kudrass, H. R. 1990. Geological results of a pre-site survey for ODP drill sites in the SE Sulu Basin. In *Proceedings of the Ocean Drilling Program, Initial Reports*, (eds. Rangin, C., Silver, E. and von Breymann, M. T.), **124**, 105-11.

Walkden, G. M. and Walkden, G. D., 1990. Cyclic sedimentation in carbonate and mixed carbonate clastic environments: four simulation programs for a desktop computer. In *Carbonate Platforms (Facies, Sequences and Evolution)*, (ed. Tucker, M. E., Wilson, J. L., Crevello, P. D., Sarg, J. F. and Read, J. F.), IAS Special Publication, **9**, 55-78.

Wilkinson, B. H., Diedrich, N. W. and Drummond, C. N. 1996. Facies successions in peritidal carbonate sequences. *Journal of Sedimentary Research*, **66**, 1065-78.

Wilkinson, B. H., Diedrich, N. W., Drummond, C. N. and Rothman, E. D. 1998. Michigan hockey, meteoric precipitation, and rhythmicity of accumulation on peritidal carbonate platforms. *Geological Society of America Bulletin*, **110**, 1075-93.

Wilkinson, B. H., Drummond, C. N., Rothman, E. D. and Diedrich, N. W. 1997. Stratal order in peritidal carbonate sequences. *Journal of Sedimentary Research*, **67**, 1068-82.

Wilson, J. L. 1972. Influence of local structure in sedimentary cycles of Beeman and Holder Formations, Sacramento Mountains, Otero County, New Mexico. In *Cyclic Sedimentation in the Permian Basin, A Symposium*, (ed. Elam, J. C. and Chuber, S.), West Texas Geological Society, Midland, TX, 100-14.

Wright, V. P. 1996. Use of palaeosols in sequence stratigraphy of peritidal carbonates. In *Sequence Stratigraphy in British Geology*, (ed. Hesselbo, S. P. and Parkinson, D. N.), Geological Society Special Publication, **103**. The Geological Society, London, 63-74.

Wright, V. P. and Vanstone, S. D. 2001. Onset of Late Palaeozoic glacio-eustasy and the evolving climates of low latitude areas: a synthesis of current understanding. *Journal of the Geological Society*, **158**, 579-82.

Figure Captions

Figure 1: Diagrammatic example of how cyclical variation in accommodation, in this case the combined effects of two sea-level curves, results in ostensibly cyclical patterns of sedimentation. Modified after Barrell (1917) and Goldhammer *et al.* (1994).

Figure 2: (a) Chronostratigraphic and (b) stratigraphic diagrams showing carbonate accumulation. The carbonate platform starts from 0m elevation and accumulates sediment according to the carbonate accumulation functions while water depth is greater than lag depth (2m). Submarine hardgrounds are created if water depth is greater than 0m but less than lag depth. If the carbonate platform is exposed (water depth less than 0) no sedimentation occurs. Sedimentation is plotted on a secondary axis with a maximum rate of 2000m Ma^{-1}. Hardgrounds and sub-aerial exposure surfaces are displayed in the appropriate chronostratigraphic position with an arbitrary y-axis value. This output from a single model run illustrates that the definition of a hierarchy is domain-dependent and that the specific characteristics of the hierarchy depend on whether it is measured in time or thickness. Both plots show the result of a single simulation run over a period of 0.4Ma producing 130m of strata.

(a) the results in time. All model time is accounted for, including time present in the thickness domain as disconformities, and so a new HFS begins when the underlying HFS ends (i.e. when the platform becomes exposed). HFSs are stacked into LFSs according to the definition presented in this study. In the time-domain, this means that a new LFS is started when a given HFS is of shorter duration than the previous HFS.

(b) the results plotted in thickness. HFSs are defined between sub-aerial exposure surfaces. LFSs are defined as stacked HFSs, beginning when a given HFS is thicker than the underlying HFS. Carbonate production rate is shown along the x-axis as a proxy for lithofacies typically depicted on stratigraphic columns from output. Large thicknesses of hardgrounds depict sedimentation occurring slightly below lag depth and outpacing sea-level rise (thus creating thin beds separated by hardgrounds).

Four LFSs are defined in the time-domain while five LFSs are defined in the thickness-domain. The difference arises during the fourth HFS which incorporates a long period of exposure and a short period of sedimentation. In the time-domain this HFS is assigned to the second LFS since it was precipitated by the second intermediate-frequency rise in sea-level in the simulation. In the thickness-domain, this third HFS is thick enough to start a new LFS, but the next HFS is also thicker than the underlying HFS, and so forms a LFS comprising a single HFS. The thickness-domain therefore gives a false impression of the actual behaviour of sea-level since it suggests five major oscillations of sea-level, when in fact there were only four.

Figure 3: (a) An example of a depth-dependent carbonate production curve used in the model.

Figure 4: Water depth history from the model depicting a 50ka interval from a single simulation run with a range of different time steps. The calculated water depths change substantially for time steps greater than 0.00005Ma (50 years) due to approximation (aliasing) error. A time-step of 0.000025Ma was chosen for the simulations as it is within the accurate range.

Figure 5: Example output of the model showing how a ratio is recorded to represent the proportion of HFSs per LFS.

(a) Chronostratigraphic diagram showing carbonate platform growth through time. For a description of the diagram refer to Figure 2.

(b) Chronostratigraphic diagram showing carbonate production and water-depth relative to a water-depth of 0m.

In this example there are three LFSs, where each successive LFS contains two, four and four HFSs. The ratio is simply the number of HFSs per LFS (1/x where x=number of HFSs) averaged over the entire simulation. In this case $h=0.33$ and would be strong evidence of the existence of a hierarchy (an average of three HFSs per LFS over the entire simulation).

Figure 6: Chronostratigraphic diagrams of simulations that resulted in a range of h-values. Amplitude of high-frequency eustatic oscillations is the only variable modified between simulations. Intermediate-frequency amplitude is fixed at 40m, run-time in all cases is 1Ma. As high-frequency oscillation amplitude increases, more HFSs are recorded and the h-value decreases. Above a high-frequency amplitude of 30m, the simulations could be said to be strongly hierarchical. Strongly hierarchical simulations do not show a strong correlation with the mean amount of total simulation time recorded as sedimentation (referred to here as preservation). The simulation with the most strongly non-hierarchical results preserves the least amount of time as sedimentation. Other simulations preserve a similar amount of time as sedimentation.

Figure 7: Stratigraphic columns of the same set of simulations shown as chronostratigraphic diagrams in Figure 6. See text for description and discussion.

Figure 8: Cumulative probability plot showing the results of 110000 model runs to evaluate the likelihood of generating a hierarchy defined in the time-domain. This plot shows that there is a 9% probability of generating a mean ratio of $h<0.5$. $h<0.5$ is taken here as weak evidence for the existence of a sedimentary hierarchy (an average of two HFSs per LFS). $h<0.33$ is taken as strong evidence of a sedimentary hierarchy (an average of three HFSs per LFS).

Using the $h<0.5$ criterion it can be said that approximately one in ten simulations (9%) display some evidence for a hierarchy in the time-domain. Using the $h<0.33$ criterion it can be said that only approximately one in twenty simulations (4%) display strong evidence for a hierarchy in the time-domain.

Figure 9: Cumulative probability plot showing the results of 110000 simulations which evaluates the likelihood of generating a hierarchy in the thickness-domain. This plot shows that there is a 15% probability of generating a mean ratio of *h*<0.5. *h*<0.5 is taken here as weak evidence for the existence of a sedimentary hierarchy (an average of two HFSs per LFS). *h*<0.33 is taken as strong evidence of a sedimentary hierarchy (an average of three HFSs per LFS).

Using the *h*<0.5 hurdle it can be said that approximately one in seven simulations (15%) display some evidence for a hierarchy in the thickness-domain. Using the *h*<0.33 hurdle it can be said that only approximately one in one hundred simulations (1%) display strong evidence for a hierarchy in the thickness-domain.

Figure 10: Scatter diagram showing the distribution of time-domain hierarchical conditions under a range of sea-level parameters. For this group of 100 simulations oscillation of low-frequency sea-level amplitude was fixed at 0m, subsidence rate was fixed at 200m Ma^{-1} and maximum production rate fixed at 2000m Ma^{-1}. Axes represent varying conditions of intermediate- and high-frequency sea-level amplitude. *h*-value (degree of hierarchy) is represented by a gradient colour-scale as depicted. (a) and (b) represent the parameter-space positions of the simulations depicted in Figure 11, where (a) is an example of a non-hierarchical simulation and (b) is an example of a hierarchical simulation. (a) and (b) have *h*-values of 0.84 and 0.43 respectively.

For a given simulation hierarchies are seen to be generated at large amplitudes of high-frequency oscillation relative to the amplitude of intermediate-frequency oscillation. This trend can generally be said to be linear. It can be said that for this set of simulations a hierarchy will be generated as long as the amplitude of high-frequency oscillation is greater than 70% of the amplitude of intermediate-oscillation.

Figure 11: Line diagram showing the distribution of time-domain mean ratio *h*-values for the simulations depicted in Figure 9. The probability of generating a sedimentary hierarchy increases with larger high-frequency amplitude. *h*-values returned from these simulations have a minimum of 0.2, which corresponds to the maximum possible number of high-frequency oscillations occurring within an intermediate-frequency oscillation. Consequently a LFS can contain a maximum of five HFSs.

Figure 12: Chronostratigraphic and stratigraphic diagrams showing (a) an example of a non-hierarchical simulation and (b) a hierarchical simulation (distinguished with a grey background). The parameter-space location of these simulations is shown in Figure 9 (a and b). Sedimentation occurs when the relative sea-level curve (RSL) has a positive elevation relative to the platform surface (represented by a 0-line) and is represented by a horizontal chronostratigraphic column showing a schematic representation of lithofacies. Per cycle, the amount of time recorded as deposition, as opposed to non-deposition during emergence, is recorded and presented as a percentage of the total duration of that cycle. This is averaged over the entire simulation and those values are presented here. It is notable that both simulations record, on average, a similar proportion of the total simulation

period. This suggests that highly hierarchical sections, even though they have more periods of sub-aerial exposure, do not record less time.

In the hierarchical example the high-frequency sea-level curve impacts much more upon the overall sea-level curve and consequently generates several HFSs per intermediate-frequency oscillation. In the non-hierarchical example, the high-frequency curve impacts less on overall sea-level behaviour due to its smaller amplitude, and therefore fewer HFSs are generated. This leads to an *h*-value of 0.43 in the hierarchical case and 0.84 in the non-hierarchical case.

Figure 13: Parameter-space plot showing the time-domain hierarchy mean ratio recorded by 10000 individual simulations. Each point represents the mean ratio for a given simulation. These points are arranged into 10x10 rectangles, the axes of which are (x) high-frequency amplitude and (y) intermediate-frequency amplitude. The squares are arranged into a trellis such that each cell of the trellis has a common low-frequency amplitude and subsidence rate. Carbonate production rate was not varied in these simulations (2000m Ma^{-1}). Platforms which drowned, and therefore never attained equilibrium relative to sea-level variation, are indicated with a different symbol. Drowning is defined by a simulation having no production other than aphotic during a single intermediate-frequency oscillation (i.e. water-depth is always greater than 55m). No results are recorded after a platform becomes drowned.

Generally, it can be said that hierarchical simulations are generated at a range of high- and intermediate-frequency amplitudes, but only at small low-frequency amplitudes (<100m) and low subsidence rates (<400m Ma^{-1}).

Figure 14: Parameter-space plot showing the thickness-domain hierarchy mean ratio recorded by 10000 individual simulations. Each point represents the mean ratio for a given simulation. These points are arranged into 10x10 rectangles, the axes of which are (x) high-frequency amplitude and (y) intermediate-frequency amplitude. The squares are arranged into a trellis such that each cell of the trellis has a common low-frequency amplitude and subsidence rate. Carbonate production rate was not varied in these simulations (2000m Ma^{-1}).

Generally, it can be said that hierarchical simulations are generated at a range of high-, intermediate- and low-frequency amplitudes, but only at low subsidence rates (<500m Ma^{-1}).

Figure 15: Representative photographs and measured sections from the two outcrop localities documented in Pollitt (2008). Outcrops are ostensibly cyclic but do not exhibit a sedimentary hierarchy when evaluated objectively. Position of measured sections on photographs is depicted with black lines. List of abbreviations: SS = sandstone, GS = grainstone, PS = packstone, WS = wackestone, BS = boundstone, MS = mudstone.

Figure 16: Line diagram showing a comparison between the mean ratio of a series of sedimentary hierarchies described by various authors and the mean ratio of the same section with the hierarchy evaluated under the strict

definition from this study. Sections indicated by a * are from Pollitt (2008). All data except those indicated by a ***** is from Lehrmann and Goldhammer (1999). Of the 93 measured outcrop sections published in Lehrmann and Goldhammer (1999), only five had an explicitly defined hierarchy (with both 5^{th}- and 4^{th}-order cycles defined).

Circles indicate the mean and mode *h-value* using the HFS and LFS definitions of the original workers. Diamonds indicate the mean and mode ratio resulting from the application of a "strict" definition of a hierarchy presented in this study (i.e. a new LFS is started when a given HFS is thicker than the last).

Using the author-defined 4^{th}-5^{th} order cycles results in a much higher ratio: <0.3, or more than three 5^{th} order cycles per 4^{th}. Using a strict definition of a hierarchy by thickness results in strongly non-hierarchical sections: average ratio of >0.6, meaning on average, less than two 5^{th} order cycles make up a 4^{th} order cycle.

Figure 17: Scatter diagram showing the mean *h*-value and number of HFSs for 88 measured sedimentary sections. Data is from Lehrmann and Goldhammer (1999). Only three measured sections have a *h*-value of <0.5 and can therefore be considered hierarchical. Furthermore, a greater degree of scatter is seen in measured sections with few HFSs. With more samples (*n*>~40), *h*-value is seen to occur in a range between 0.6 and 0.7. Short sedimentary sections with few interpreted HFSs may therefore give a false impression of a sedimentary hierarchy.

Figure 18: Scatter diagram showing the relationship between the number of HFSs in an outcrop section and the mean *h*-value of that section. Data is from Lehrmann and Goldhammer (1999). The amount of scatter in *h*-value decreases as the number of recorded HFSs increases. The amount of scatter associated with fewer HFSs suggests these sections are under-sampled. This plot suggests that to accurately determine the degree of hierarchy inherent to a stratigraphic section that section should have >~20 HFSs.

Figure 19: Line chart showing the mean and mode "run" of bed thickness per outcrop from data in Lehrmann and Goldhammer (1999). For example, a series of thinning upwards beds with the consecutive thickness; 4m, 3m, 2m, 1m, 4m, would constitute a run of four. Error bars represent the standard distribution of the mean number of beds per HFS for that outcrop.

Table 1: Model parameters used. In each simulation parameters were varied within a range according to a stepping value. All simulations had a run time of 3Ma. Maximum oligophotic and aphotic production rates were modelled as a proportion of the maximum euphotic rate (20% and 5% respectively). Lag depth was fixed at 2m. In order to evaluate the interaction of all possible parameter permutations, 110000 simulations were conducted.

Figure 1

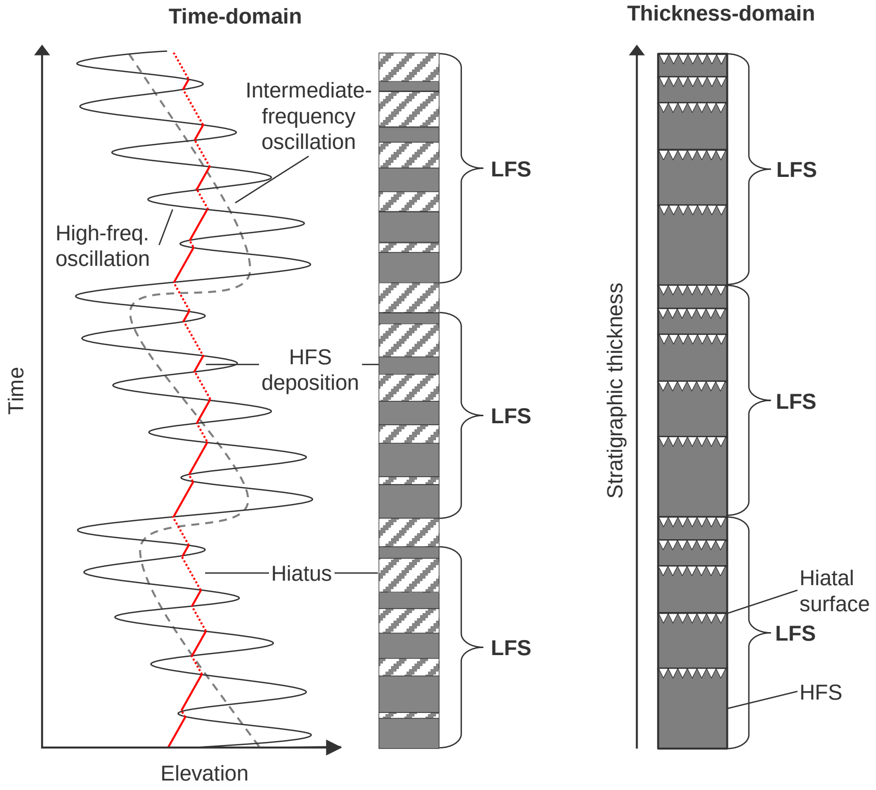

Time-domain
Thickness-domain
Intermediate-frequency oscillation
High-freq. oscillation
HFS deposition
Hiatus
LFS
LFS
LFS
Time
Elevation
Stratigraphic thickness
LFS
LFS
LFS
Hiatal surface
HFS

Figure 2

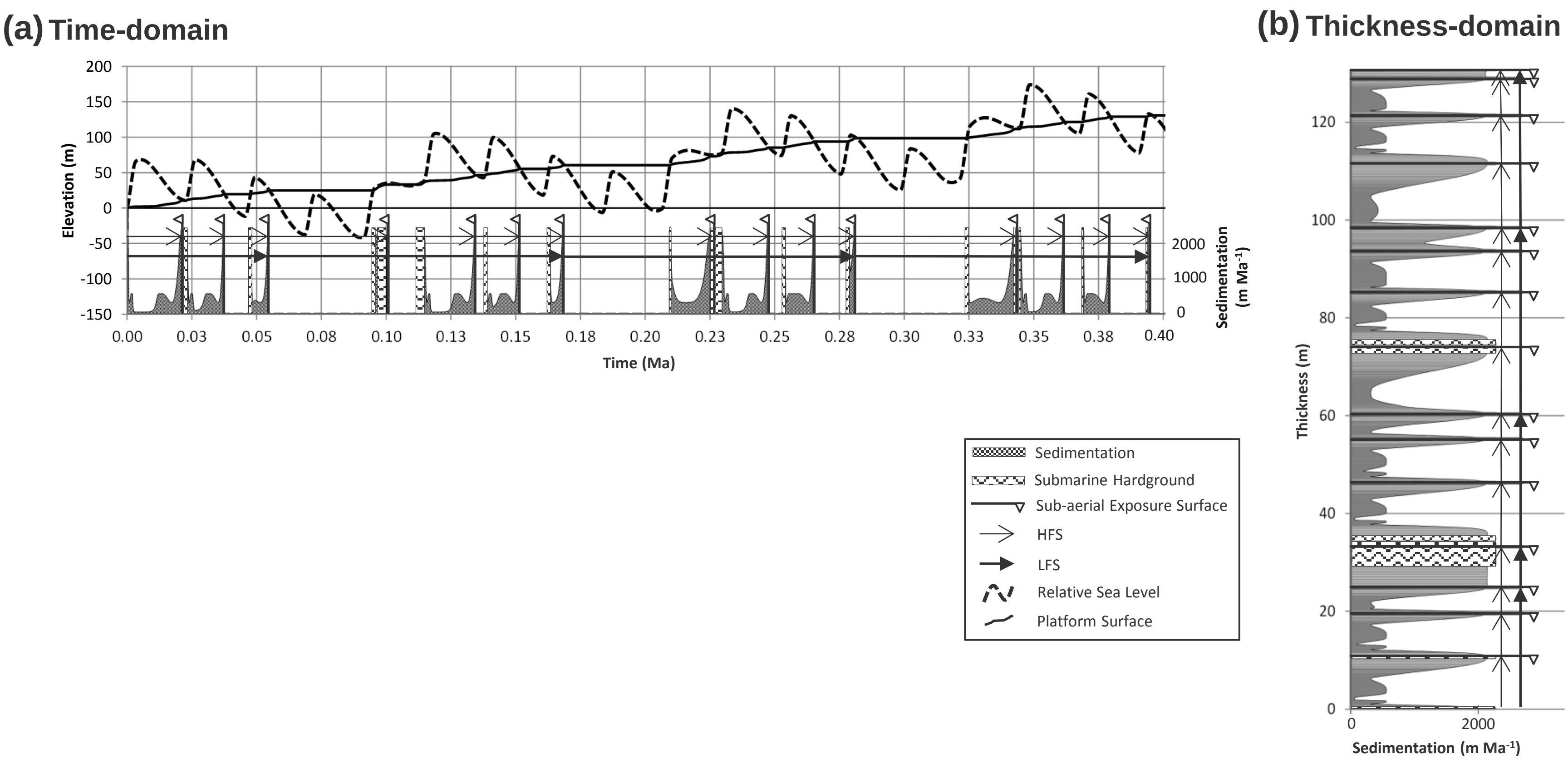

(a) Time-domain
(b) Thickness-domain
Elevation (m)
Time (Ma)
Sedimentation (m Ma-1)
Thickness (m)
Sedimentation
Submarine Hardground
Sub-aerial Exposure Surface
HFS
LFS
Relative Sea Level
Platform Surface

Figure 3

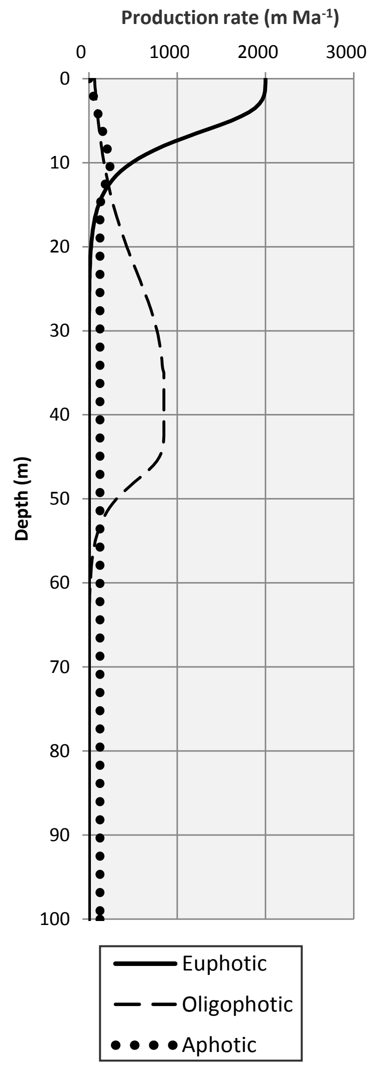
Production rate (m Ma^{-1})
0
1000
2000
3000
0
10
20
30
40
50
60
70
80
90
100
Depth (m)
Euphotic
Oligophotic
Aphotic

Figure 4

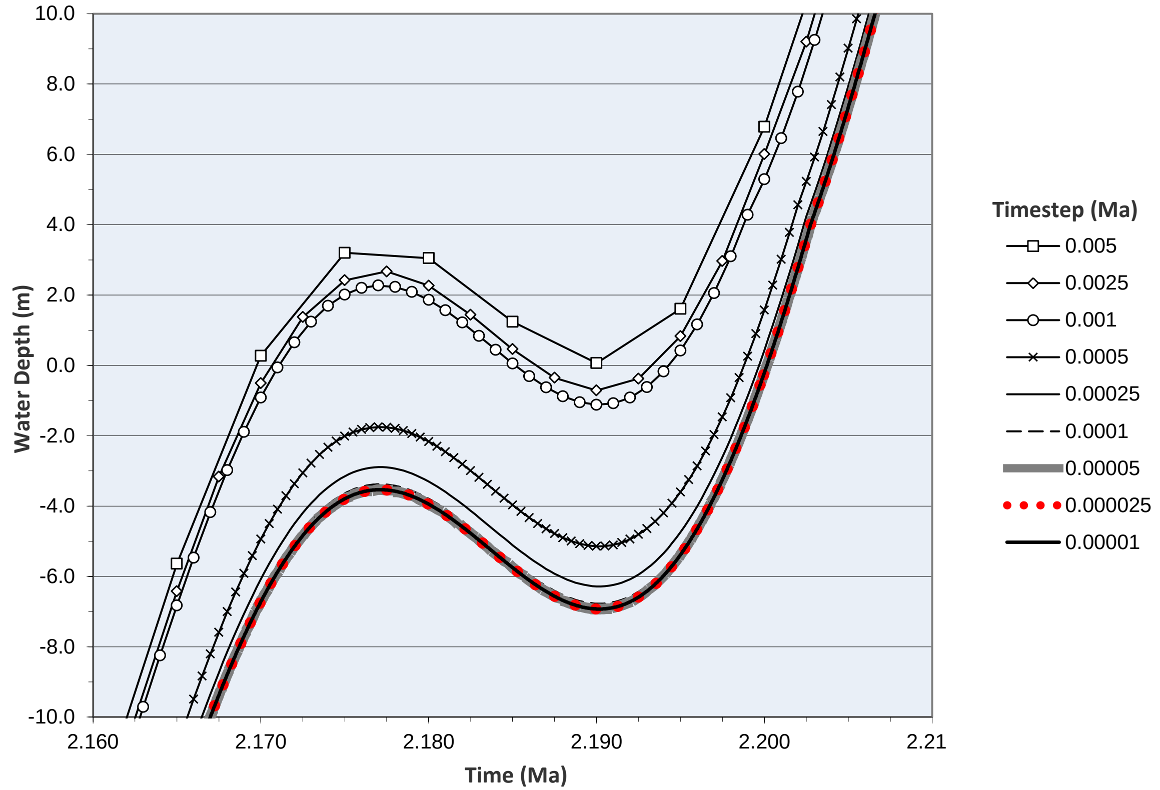

Water Depth (m)
10.0
8.0
6.0
4.0
2.0
0.0
-2.0
-4.0
-6.0
-8.0
-10.0
2.160
2.170
2.180
2.190
2.200
2.21
Time (Ma)
Timestep (Ma)
0.005
0.0025
0.001
0.0005
0.00025
0.0001
0.00005
0.000025
0.00001

Figure 5

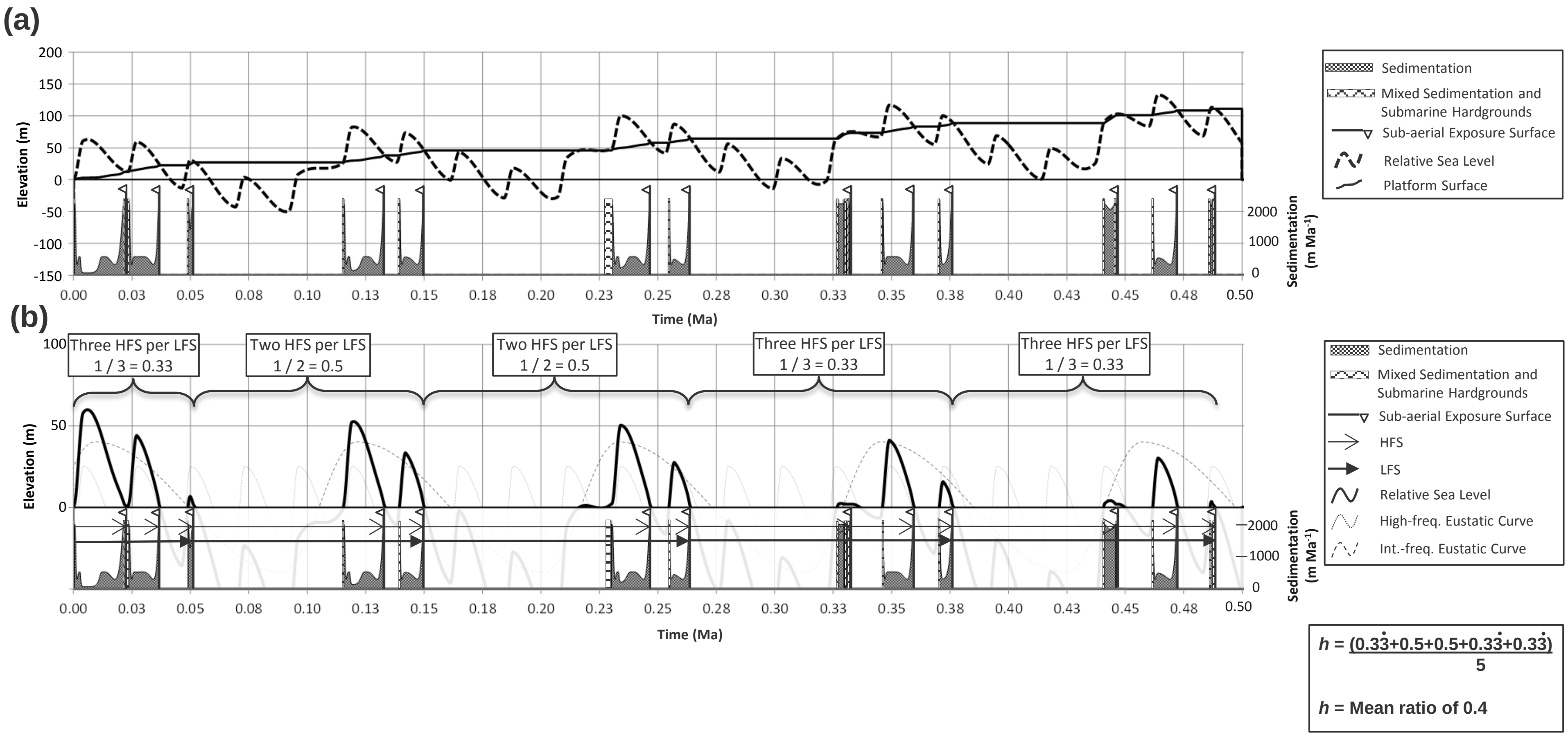
(a)
Elevation (m)
Sedimentation (m Ma-1)
Time (Ma)
Sedimentation
Mixed Sedimentation and Submarine Hardgrounds
Sub-aerial Exposure Surface
Relative Sea Level
Platform Surface
(b)
Three HFS per LFS
1 / 3 = 0.33
Two HFS per LFS
1 / 2 = 0.5
Two HFS per LFS
1 / 2 = 0.5
Three HFS per LFS
1 / 3 = 0.33
Three HFS per LFS
1 / 3 = 0.33
Elevation (m)
Sedimentation (m Ma-1)
Time (Ma)
Sedimentation
Mixed Sedimentation and Submarine Hardgrounds
Sub-aerial Exposure Surface
HFS
LFS
Relative Sea Level
High-freq. Eustatic Curve
Int.-freq. Eustatic Curve
h = (0.33+0.5+0.5+0.33+0.33) / 5
h = Mean ratio of 0.4

Figure 6

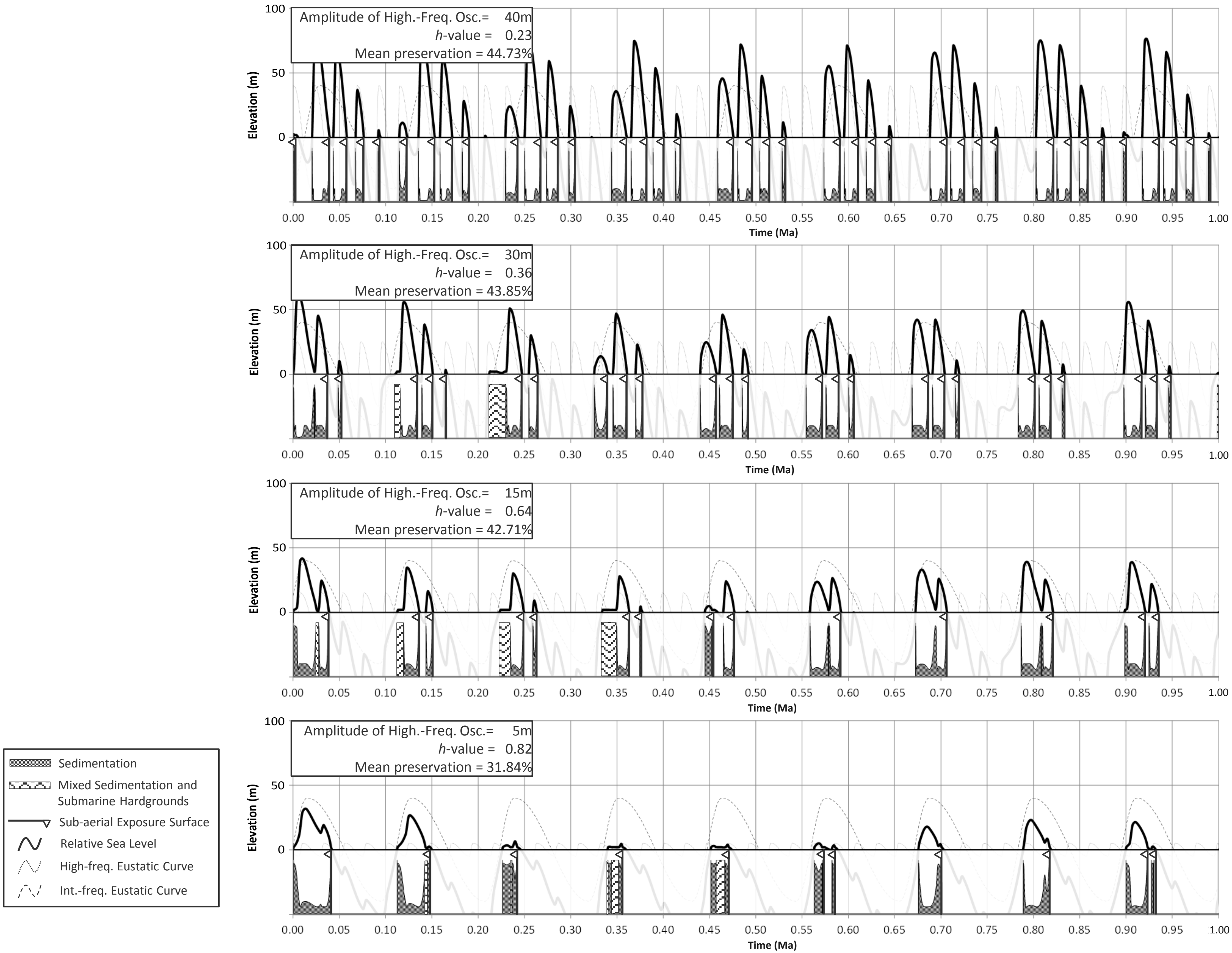
Amplitude of High.-Freq. Osc.= 40m
h-value = 0.23
Mean preservation = 44.73%
Amplitude of High.-Freq. Osc.= 30m
h-value = 0.36
Mean preservation = 43.85%
Amplitude of High.-Freq. Osc.= 15m
h-value = 0.64
Mean preservation = 42.71%
Amplitude of High.-Freq. Osc.= 5m
h-value = 0.82
Mean preservation = 31.84%
Elevation (m)
Time (Ma)
100
50
0
0.00
0.05
0.10
0.15
0.20
0.25
0.30
0.35
0.40
0.45
0.50
0.55
0.60
0.65
0.70
0.75
0.80
0.85
0.90
0.95
1.00
Sedimentation
Mixed Sedimentation and Submarine Hardgrounds
Sub-aerial Exposure Surface
Relative Sea Level
High-freq. Eustatic Curve
Int.-freq. Eustatic Curve

Figure 7

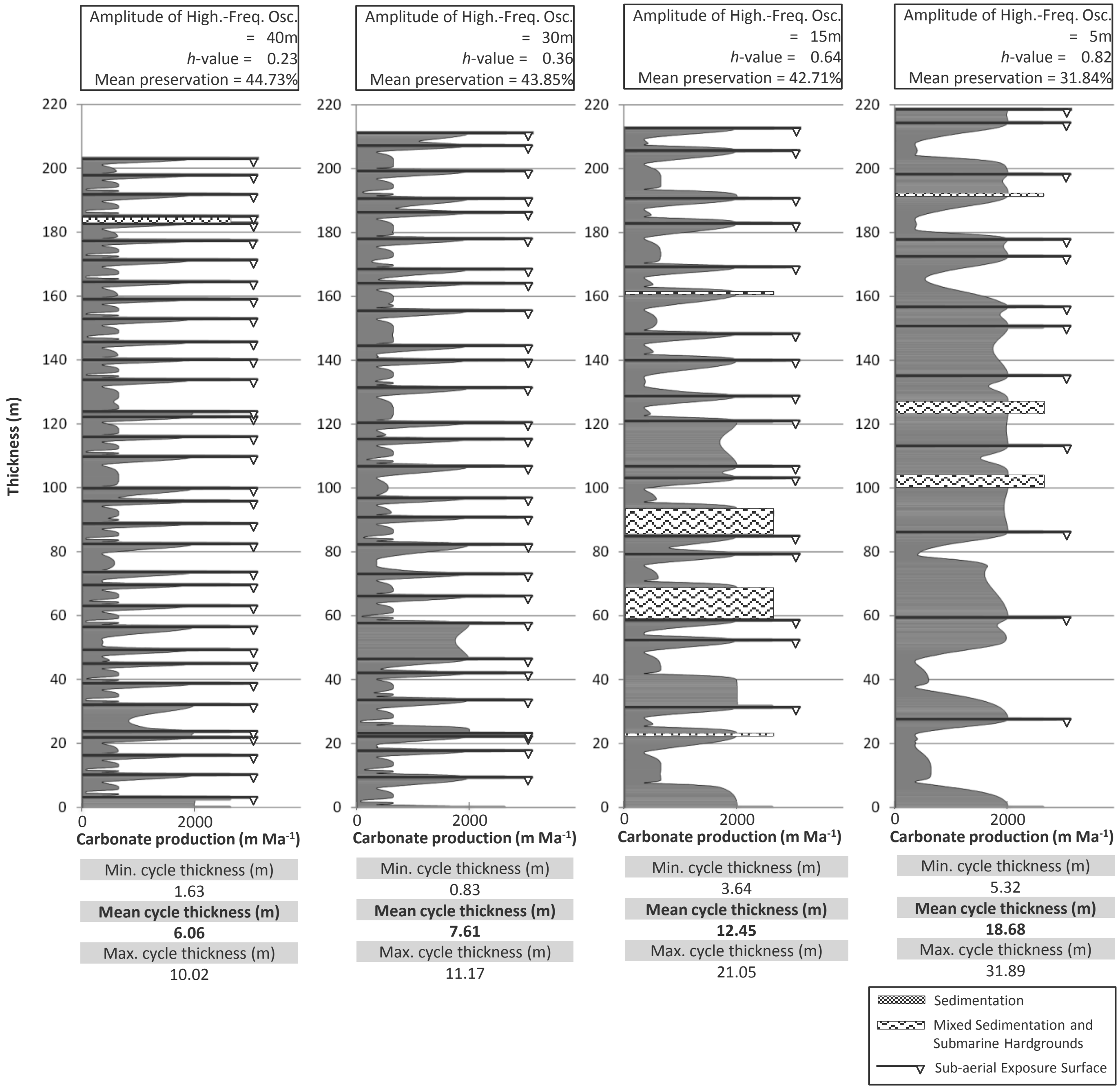

Amplitude of High.-Freq. Osc. = 40m
h-value = 0.23
Mean preservation = 44.73%
Amplitude of High.-Freq. Osc. = 30m
h-value = 0.36
Mean preservation = 43.85%
Amplitude of High.-Freq. Osc. = 15m
h-value = 0.64
Mean preservation = 42.71%
Amplitude of High.-Freq. Osc. = 5m
h-value = 0.82
Mean preservation = 31.84%
Thickness (m)
0
20
40
60
80
100
120
140
160
180
200
220
0
2000
Carbonate production (m Ma-1)
Min. cycle thickness (m)
1.63
Mean cycle thickness (m)
6.06
Max. cycle thickness (m)
10.02
Min. cycle thickness (m)
0.83
Mean cycle thickness (m)
7.61
Max. cycle thickness (m)
11.17
Min. cycle thickness (m)
3.64
Mean cycle thickness (m)
12.45
Max. cycle thickness (m)
21.05
Min. cycle thickness (m)
5.32
Mean cycle thickness (m)
18.68
Max. cycle thickness (m)
31.89
Sedimentation
Mixed Sedimentation and Submarine Hardgrounds
Sub-aerial Exposure Surface

Figure 8

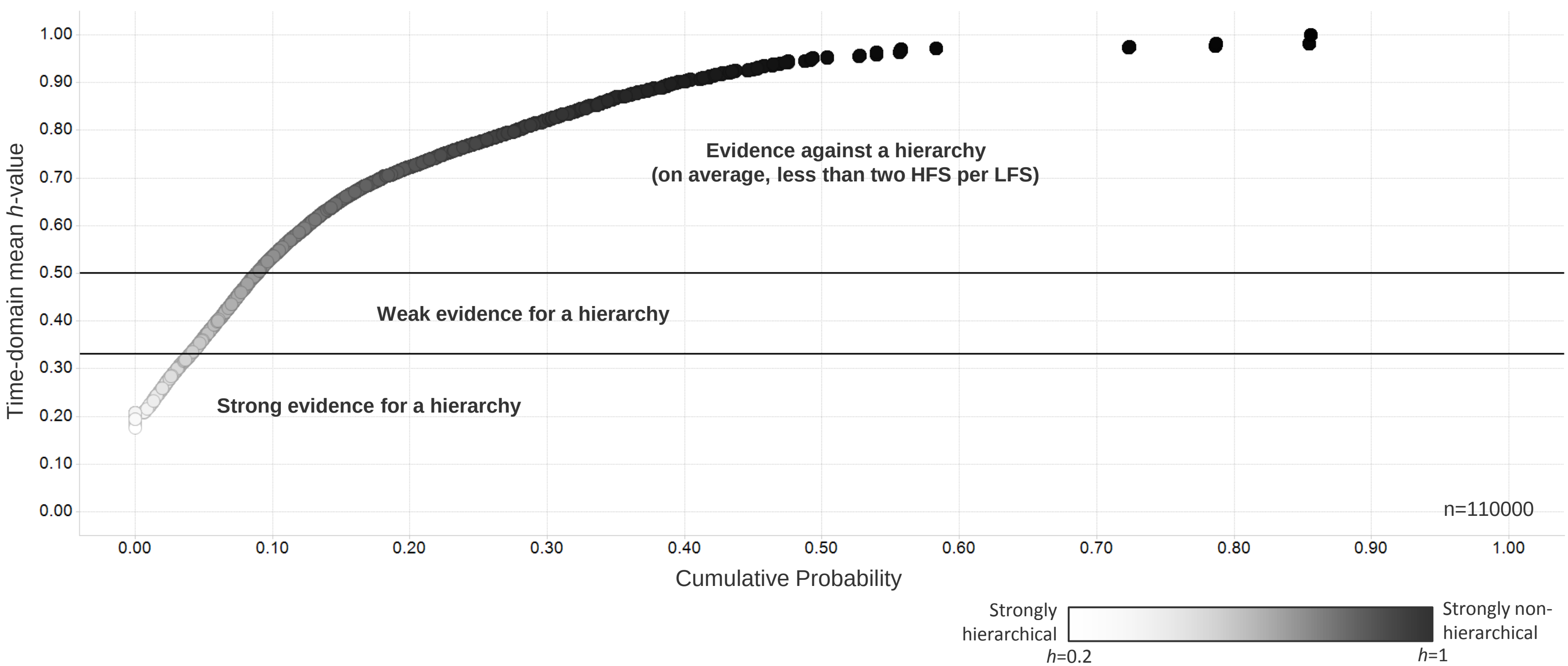

Time-domain mean h-value
1.00
0.90
0.80
0.70
0.60
0.50
0.40
0.30
0.20
0.10
0.00
Evidence against a hierarchy
(on average, less than two HFS per LFS)
Weak evidence for a hierarchy
Strong evidence for a hierarchy
n=110000
0.00
0.10
0.20
0.30
0.40
0.50
0.60
0.70
0.80
0.90
1.00
Cumulative Probability
Strongly hierarchical
h=0.2
Strongly non-hierarchical
h=1

Figure 9

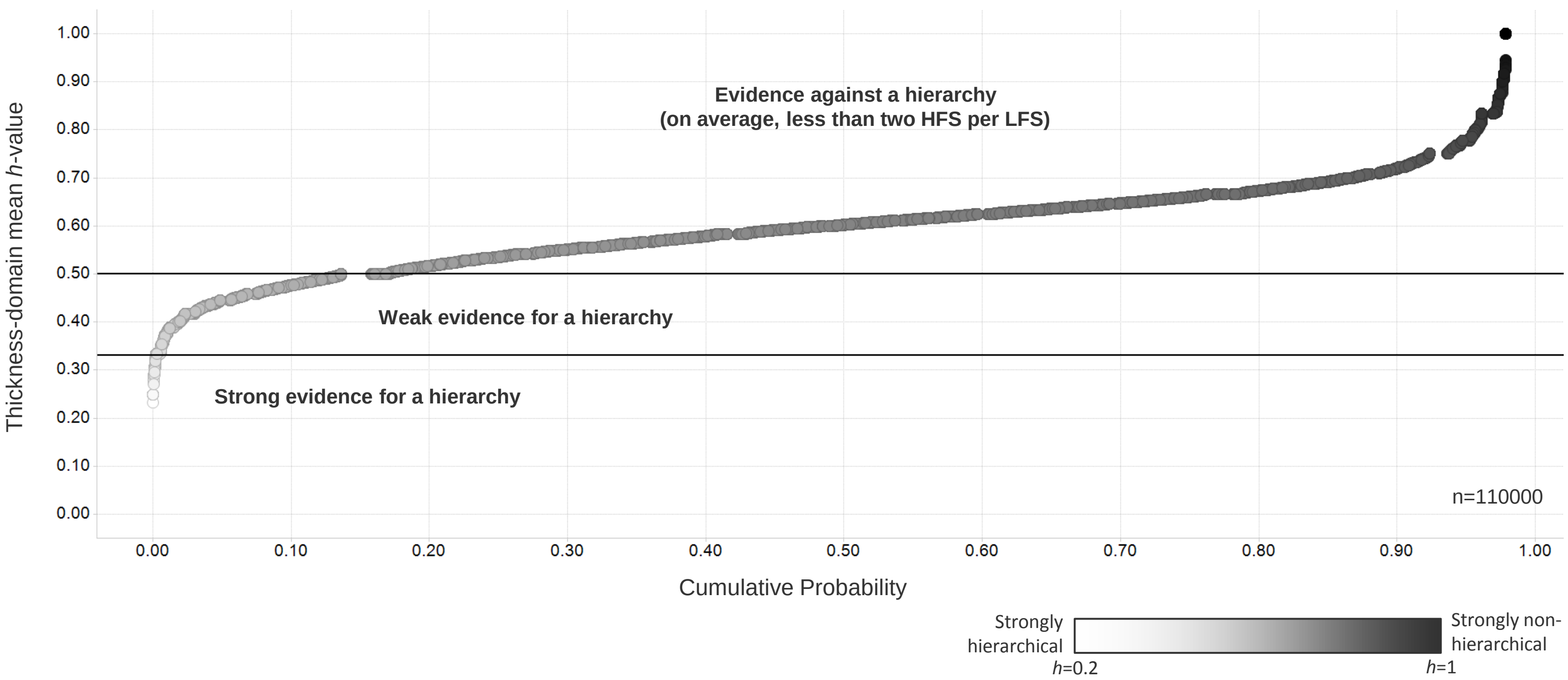

Evidence against a hierarchy
(on average, less than two HFS per LFS)
Weak evidence for a hierarchy
Strong evidence for a hierarchy
Thickness-domain mean h-value
1.00
0.90
0.80
0.70
0.60
0.50
0.40
0.30
0.20
0.10
0.00
0.00
0.10
0.20
0.30
0.40
0.50
0.60
0.70
0.80
0.90
1.00
Cumulative Probability
n=110000
Strongly hierarchical
Strongly non-hierarchical
h=0.2
h=1

Figure 10

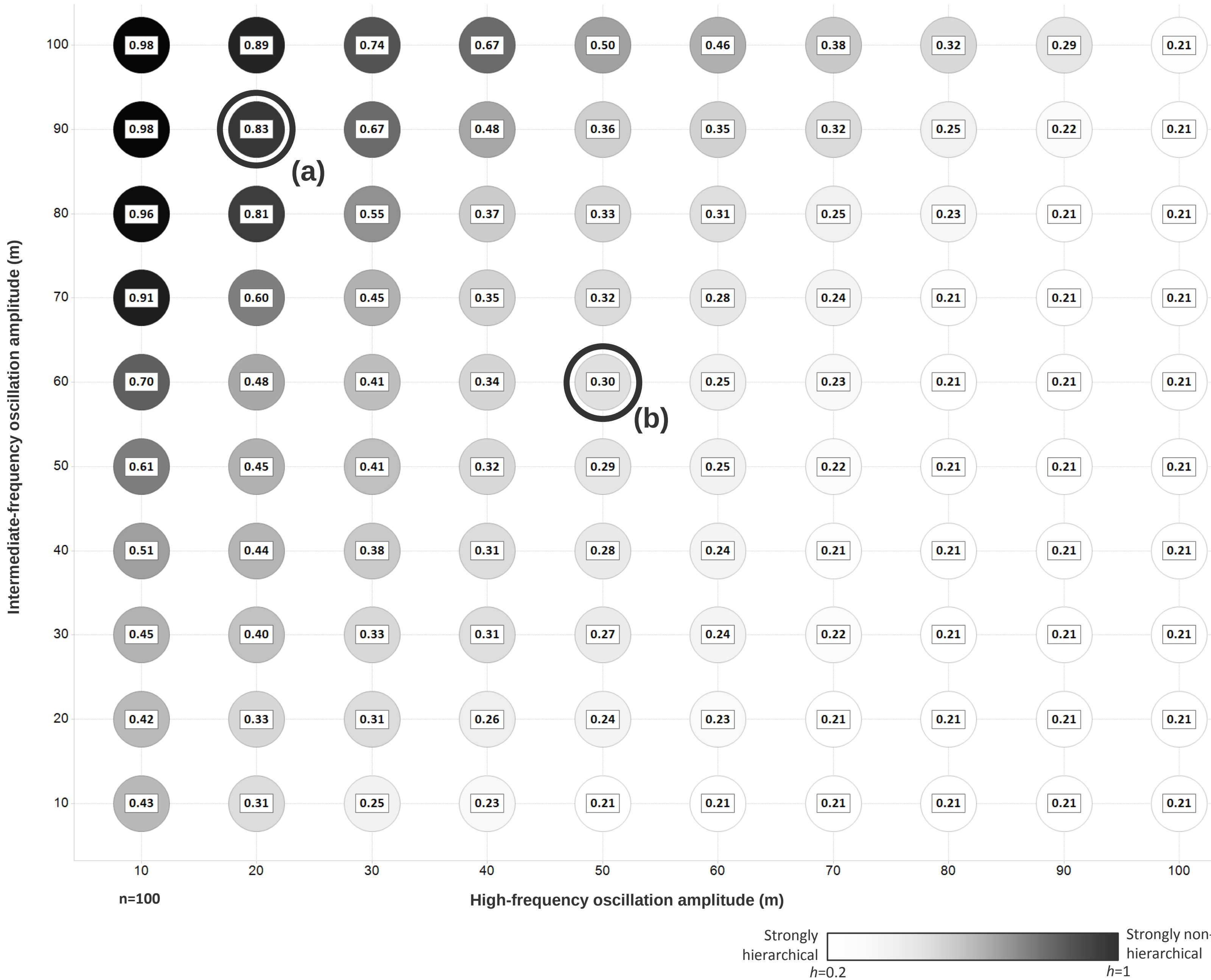

Intermediate-frequency oscillation amplitude (m)
100 0.98 0.89 0.74 0.67 0.50 0.46 0.38 0.32 0.29 0.21
90 0.98 0.83 0.67 0.48 0.36 0.35 0.32 0.25 0.22 0.21
80 0.96 0.81 0.55 0.37 0.33 0.31 0.25 0.23 0.21 0.21
70 0.91 0.60 0.45 0.35 0.32 0.28 0.24 0.21 0.21 0.21
60 0.70 0.48 0.41 0.34 0.30 0.25 0.23 0.21 0.21 0.21
50 0.61 0.45 0.41 0.32 0.29 0.25 0.22 0.21 0.21 0.21
40 0.51 0.44 0.38 0.31 0.28 0.24 0.21 0.21 0.21 0.21
30 0.45 0.40 0.33 0.31 0.27 0.24 0.22 0.21 0.21 0.21
20 0.42 0.33 0.31 0.26 0.24 0.23 0.21 0.21 0.21 0.21
10 0.43 0.31 0.25 0.23 0.21 0.21 0.21 0.21 0.21 0.21
(a)
(b)
10 20 30 40 50 60 70 80 90 100
n=100
High-frequency oscillation amplitude (m)
Strongly hierarchical
h=0.2
Strongly non-hierarchical
h=1

Figure 11

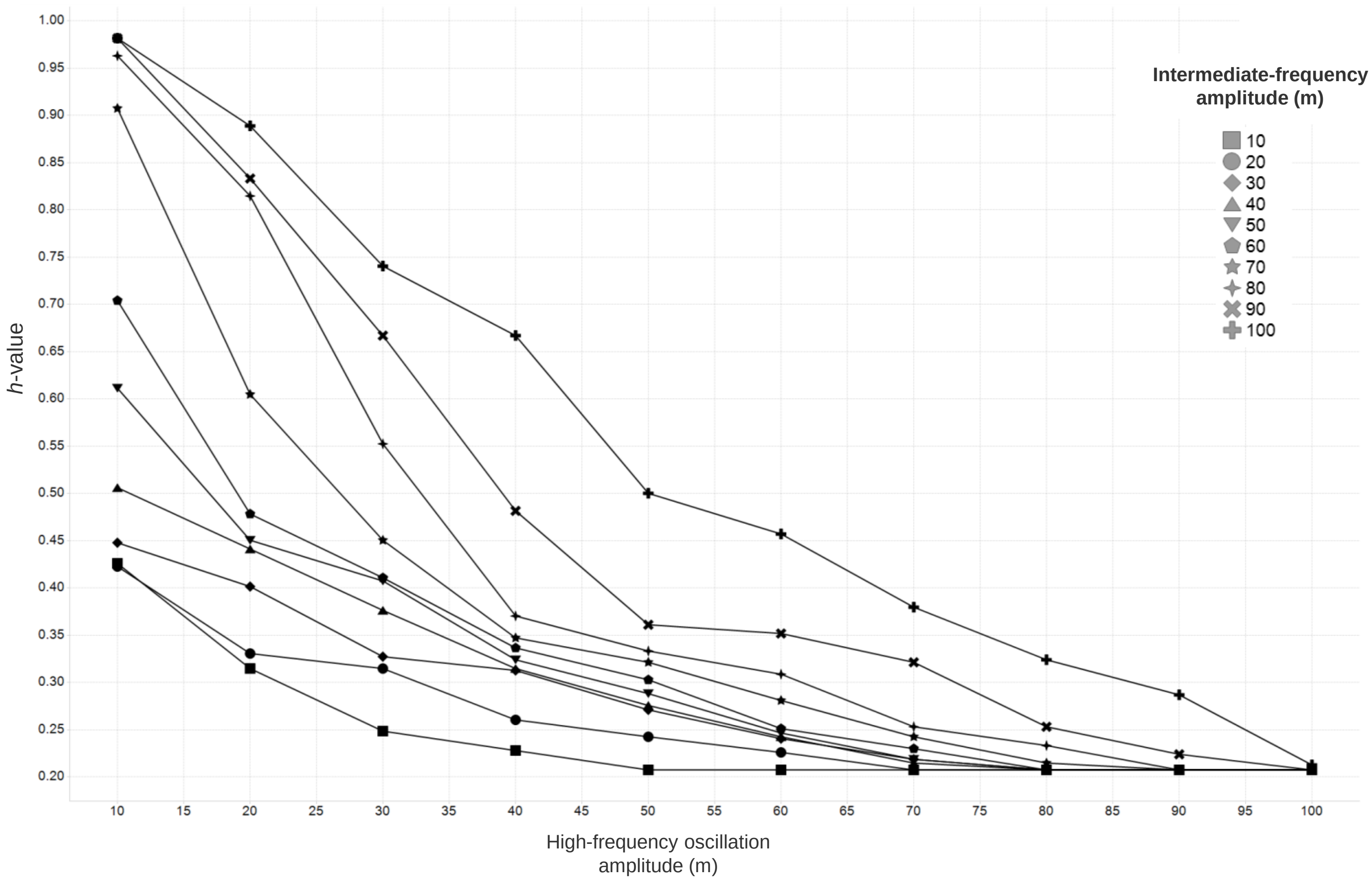

1.00
0.95
0.90
0.85
0.80
0.75
0.70
0.65
0.60
0.55
0.50
0.45
0.40
0.35
0.30
0.25
0.20
h-value
10
15
20
25
30
35
40
45
50
55
60
65
70
75
80
85
90
95
100
High-frequency oscillation amplitude (m)
Intermediate-frequency amplitude (m)
10
20
30
40
50
60
70
80
90
100

Figure 12

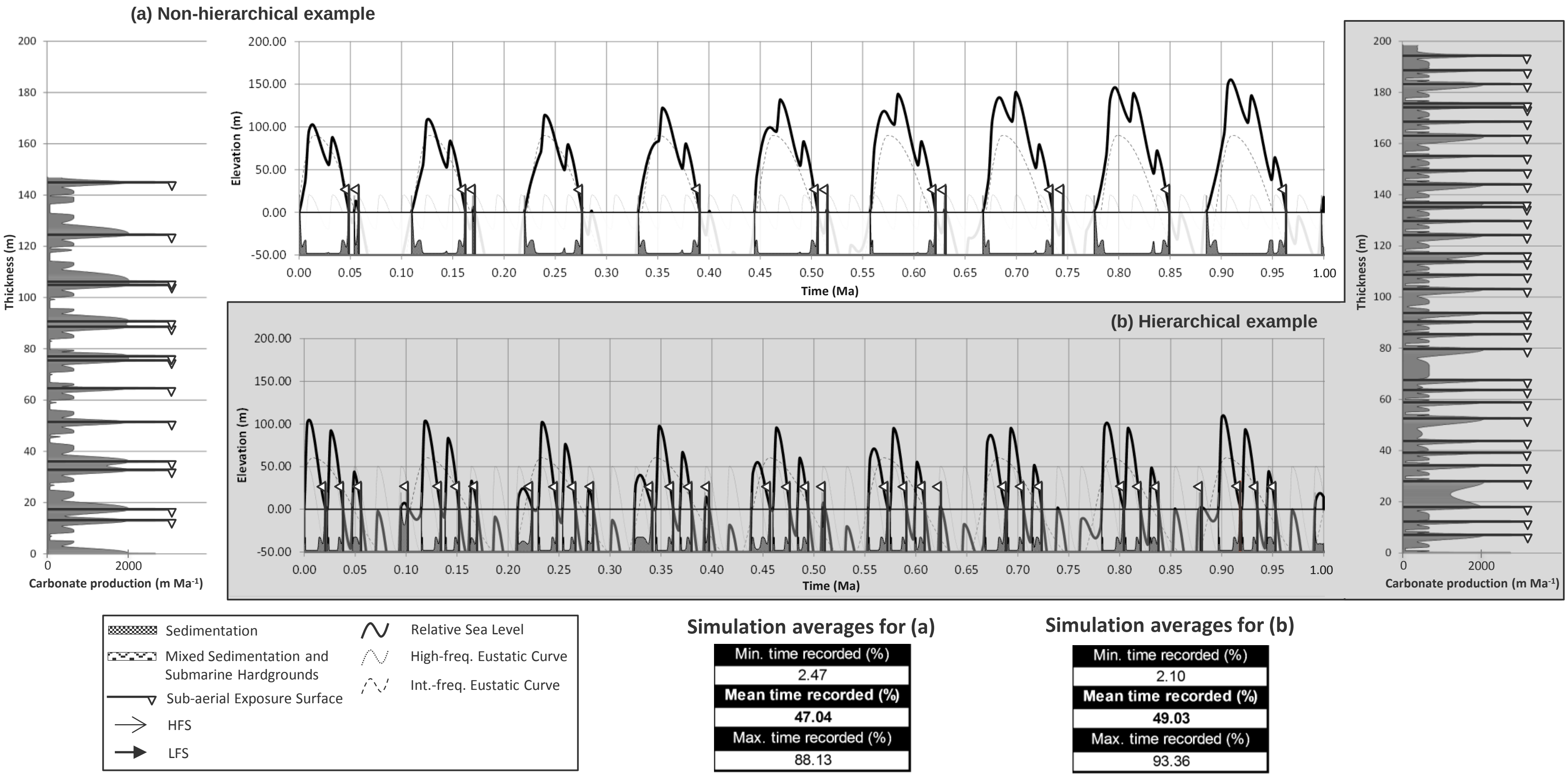

Simulation averages for (a)

Min. time recorded (%)
2.47
Mean time recorded (%)
47.04
Max. time recorded (%)
88.13

Simulation averages for (b)

Min. time recorded (%)
2.10
Mean time recorded (%)
49.03
Max. time recorded (%)
93.36

Figure 13

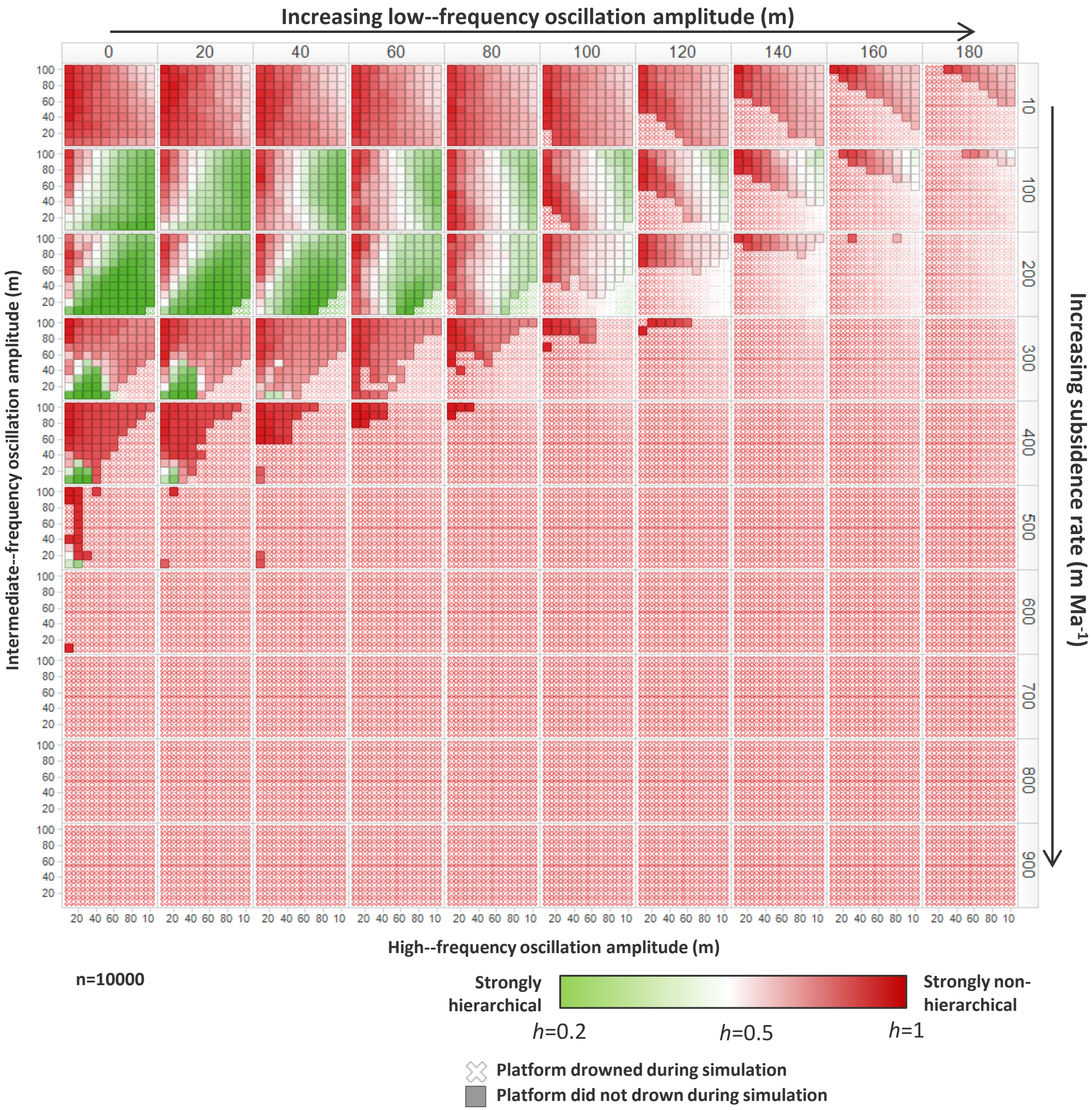

Increasing low--frequency oscillation amplitude (m)
0
20
40
60
80
100
120
140
160
180
Intermediate--frequency oscillation amplitude (m)
Increasing subsidence rate (m Ma-1)
10
100
200
300
400
500
600
700
800
900
High--frequency oscillation amplitude (m)
n=10000
Strongly hierarchical
Strongly non-hierarchical
h=0.2
h=0.5
h=1
Platform drowned during simulation
Platform did not drown during simulation

Figure 14

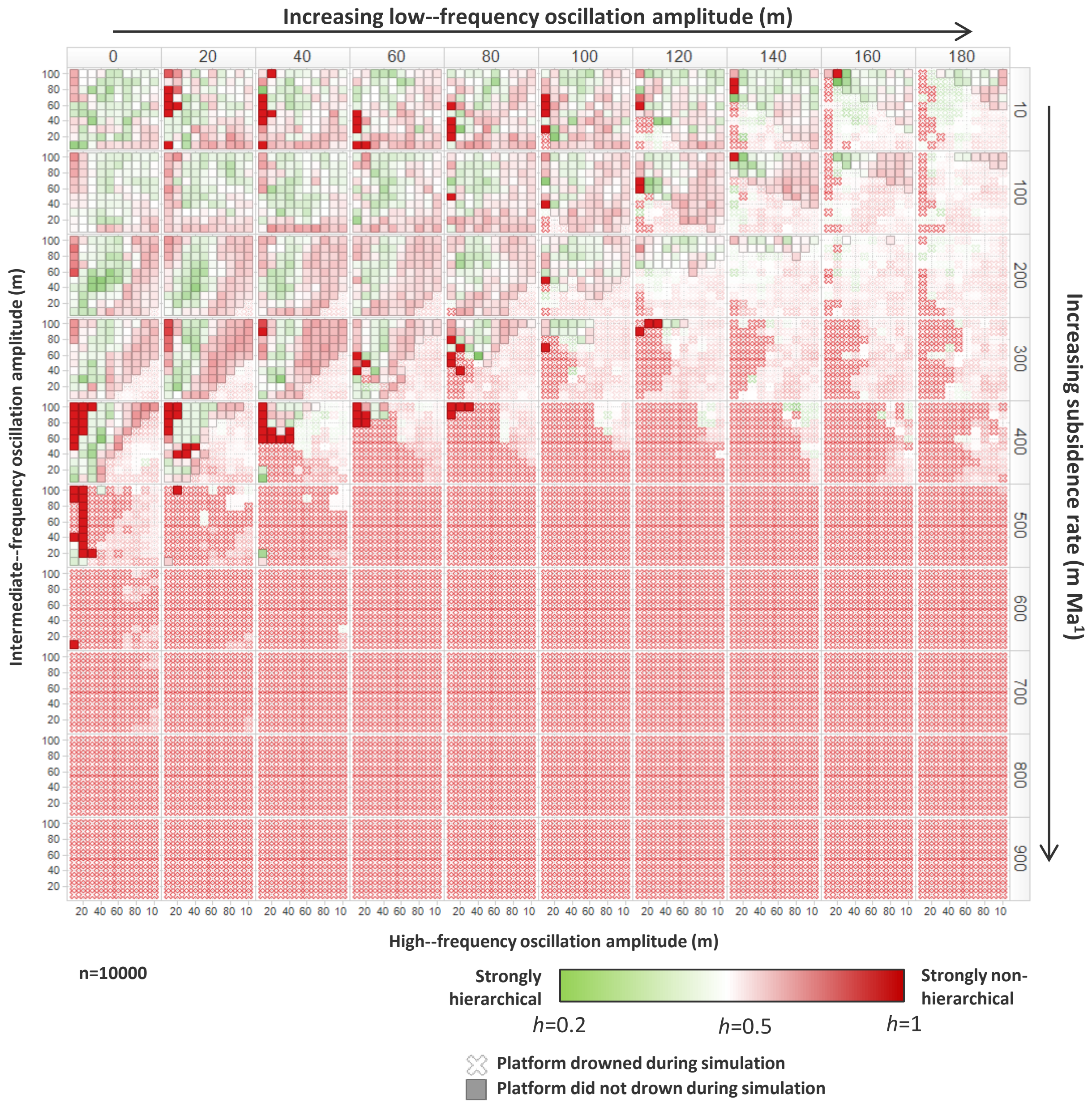
Increasing low--frequency oscillation amplitude (m)
0
20
40
60
80
100
120
140
160
180
Intermediate--frequency oscillation amplitude (m)
100
80
60
40
20
10
100
200
300
400
500
600
700
800
900
Increasing subsidence rate (m Ma^{-1})
20 40 60 80 10
High--frequency oscillation amplitude (m)
n=10000
Strongly hierarchical
Strongly non-hierarchical
h=0.2
h=0.5
h=1
Platform drowned during simulation
Platform did not drown during simulation

Figure 15

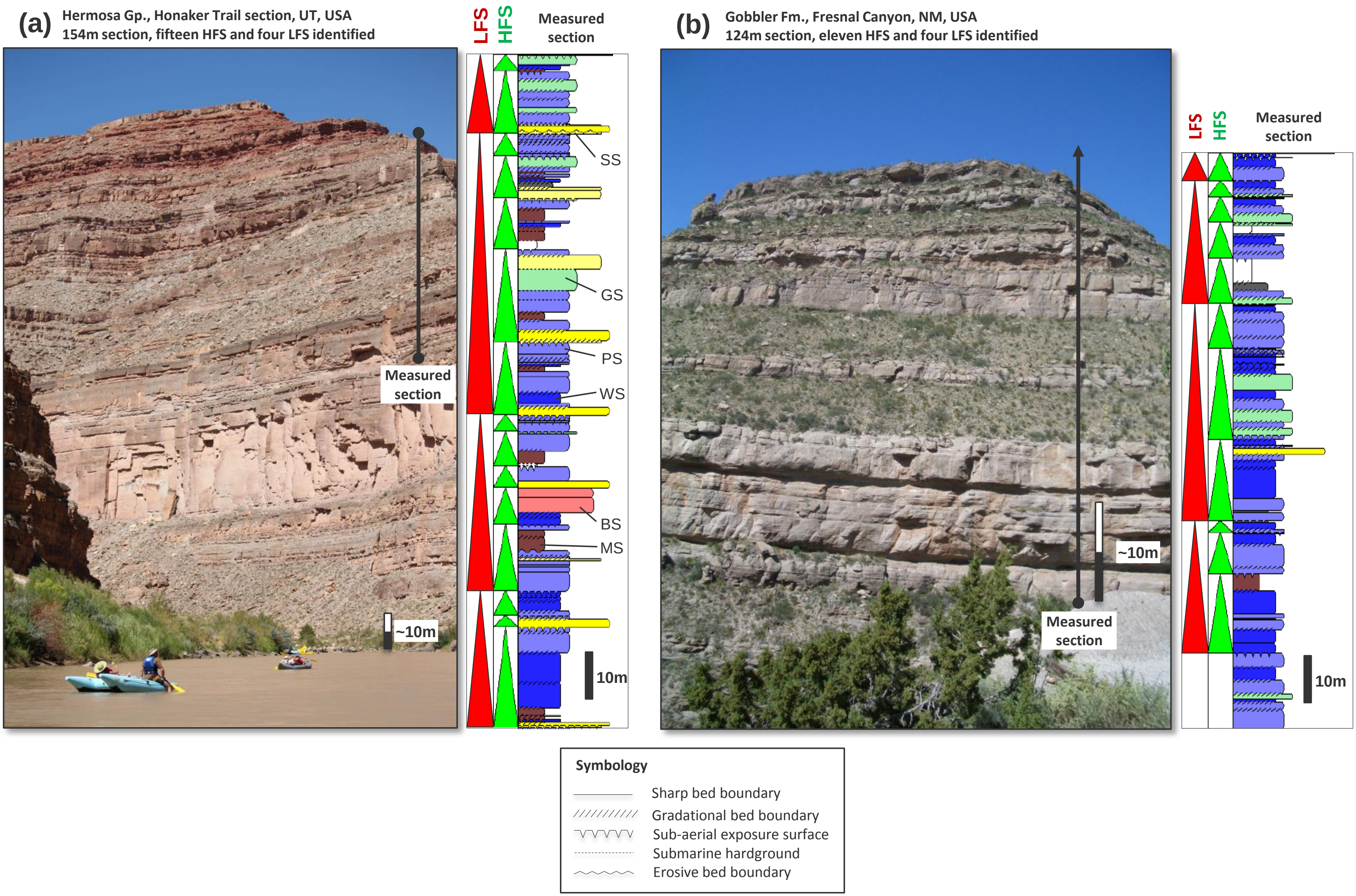
(a)
Hermosa Gp., Honaker Trail section, UT, USA
154m section, fifteen HFS and four LFS identified
LFS
HFS
Measured section
SS
GS
PS
WS
BS
MS
10m
~10m
Measured section
(b)
Gobbler Fm., Fresnal Canyon, NM, USA
124m section, eleven HFS and four LFS identified
LFS
HFS
Measured section
~10m
Measured section
10m
Symbology
Sharp bed boundary
Gradational bed boundary
Sub-aerial exposure surface
Submarine hardground
Erosive bed boundary

Figure 16

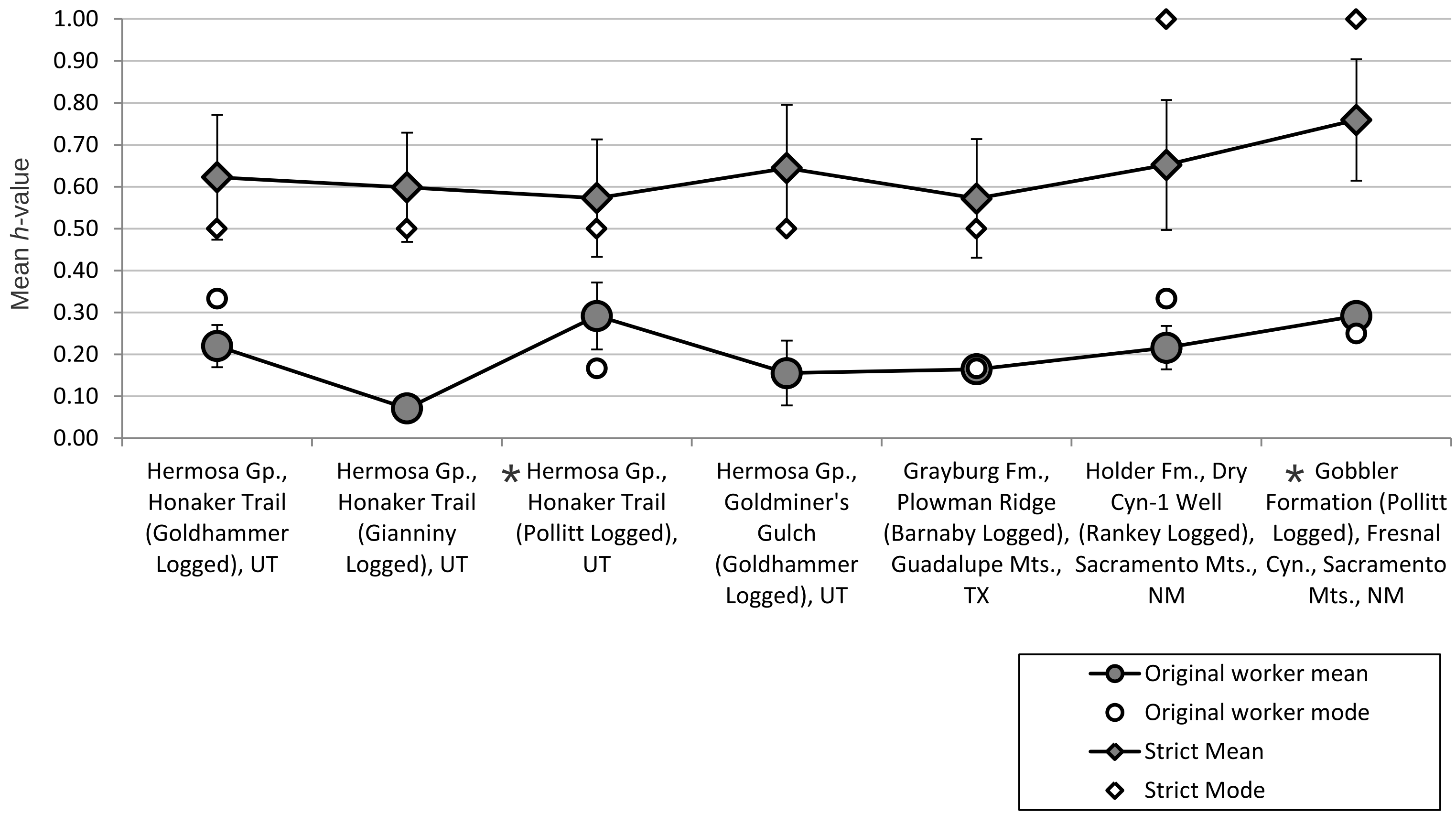

1.00
0.90
0.80
0.70
0.60
0.50
0.40
0.30
0.20
0.10
0.00
Mean h-value
Hermosa Gp., Honaker Trail (Goldhammer Logged), UT
Hermosa Gp., Honaker Trail (Gianniny Logged), UT
* Hermosa Gp., Honaker Trail (Pollitt Logged), UT
Hermosa Gp., Goldminer's Gulch (Goldhammer Logged), UT
Grayburg Fm., Plowman Ridge (Barnaby Logged), Guadalupe Mts., TX
Holder Fm., Dry Cyn-1 Well (Rankey Logged), Sacramento Mts., NM
* Gobbler Formation (Pollitt Logged), Fresnal Cyn., Sacramento Mts., NM
Original worker mean
Original worker mode
Strict Mean
Strict Mode

Figure 17

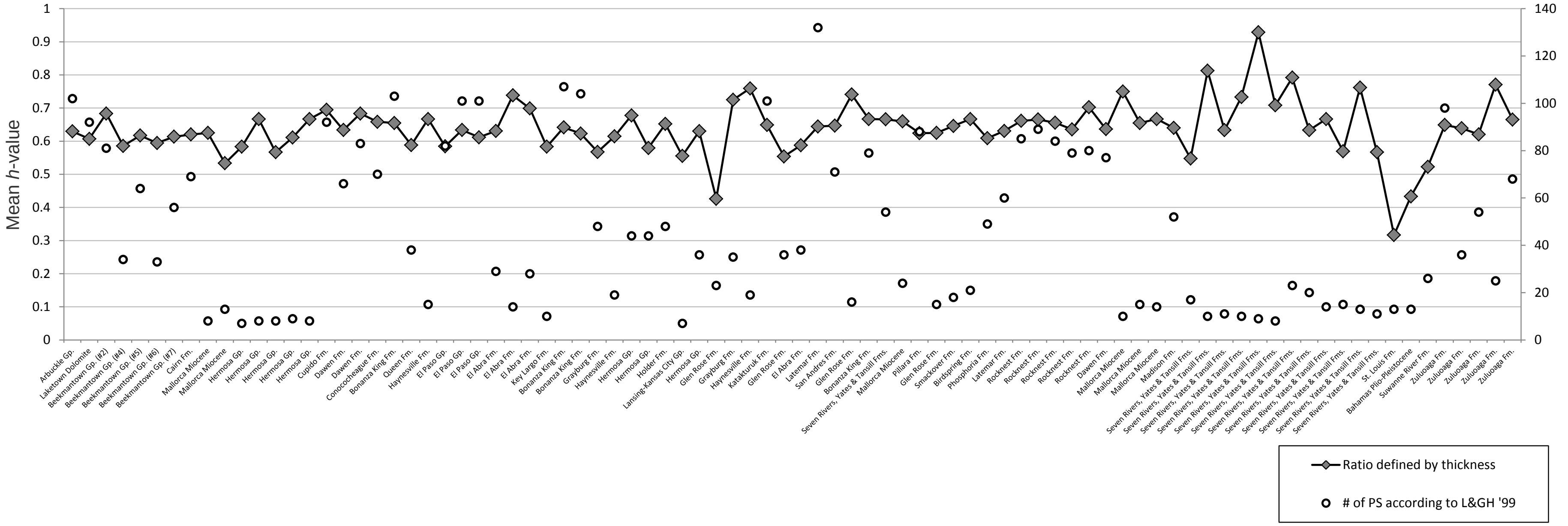

Mean *h*-value
Number of HFS
1
0.9
0.8
0.7
0.6
0.5
0.4
0.3
0.2
0.1
0
140
120
100
80
60
40
20
0
Arbuckle Gp.
Laketown Dolomite
Beekmantown Gp. (#2)
Beekmantown Gp. (#4)
Beekmantown Gp. (#5)
Beekmantown Gp. (#6)
Beekmantown Gp. (#7)
Cairn Fm.
Mallorca Miocene
Mallorca Miocene
Hermosa Gp.
Hermosa Gp.
Hermosa Gp.
Hermosa Gp.
Hermosa Gp.
Cupido Fm.
Dawen Fm.
Dawen Fm.
Conococheague Fm.
Bonanza King Fm.
Queen Fm.
Haynesville Fm.
El Paso Gp.
El Paso Gp.
El Paso Gp.
El Abra Fm.
El Abra Fm.
El Abra Fm.
Key Largo Fm.
Bonanza King Fm.
Bonanza King Fm.
Grayburg Fm.
Haynesville Fm.
Hermosa Gp.
Hermosa Gp.
Holder Fm.
Lansing-Kansas City Gp.
Hermosa Gp.
Glen Rose Fm.
Grayburg Fm.
Haynesville Fm.
Katakturuk Fm.
Glen Rose Fm.
El Abra Fm.
Latemar Fm.
San Andres Fm.
Glen Rose Fm.
Bonanza King Fm.
Seven Rivers, Yates & Tansill Fms.
Mallorca Miocene
Pillara Fm.
Glen Rose Fm.
Smackover Fm.
Birdspring Fm.
Phosphoria Fm.
Latemar Fm.
Rocknest Fm.
Rocknest Fm.
Rocknest Fm.
Rocknest Fm.
Rocknest Fm.
Dawen Fm.
Mallorca Miocene
Mallorca Miocene
Mallorca Miocene
Madison Fm.
Seven Rivers, Yates & Tansill Fms.
Seven Rivers, Yates & Tansill Fms.
Seven Rivers, Yates & Tansill Fms.
Seven Rivers, Yates & Tansill Fms.
Seven Rivers, Yates & Tansill Fms.
Seven Rivers, Yates & Tansill Fms.
Seven Rivers, Yates & Tansill Fms.
Seven Rivers, Yates & Tansill Fms.
Seven Rivers, Yates & Tansill Fms.
Seven Rivers, Yates & Tansill Fms.
St. Louis Fm.
Bahamas Plio-Pleistocene
Suwanne River Fm.
Zuluoaga Fm.
Zuluoaga Fm.
Zuluoaga Fm.
Zuluoaga Fm.
Zuluoaga Fm.
Ratio defined by thickness
# of PS according to L&GH '99

Figure 18

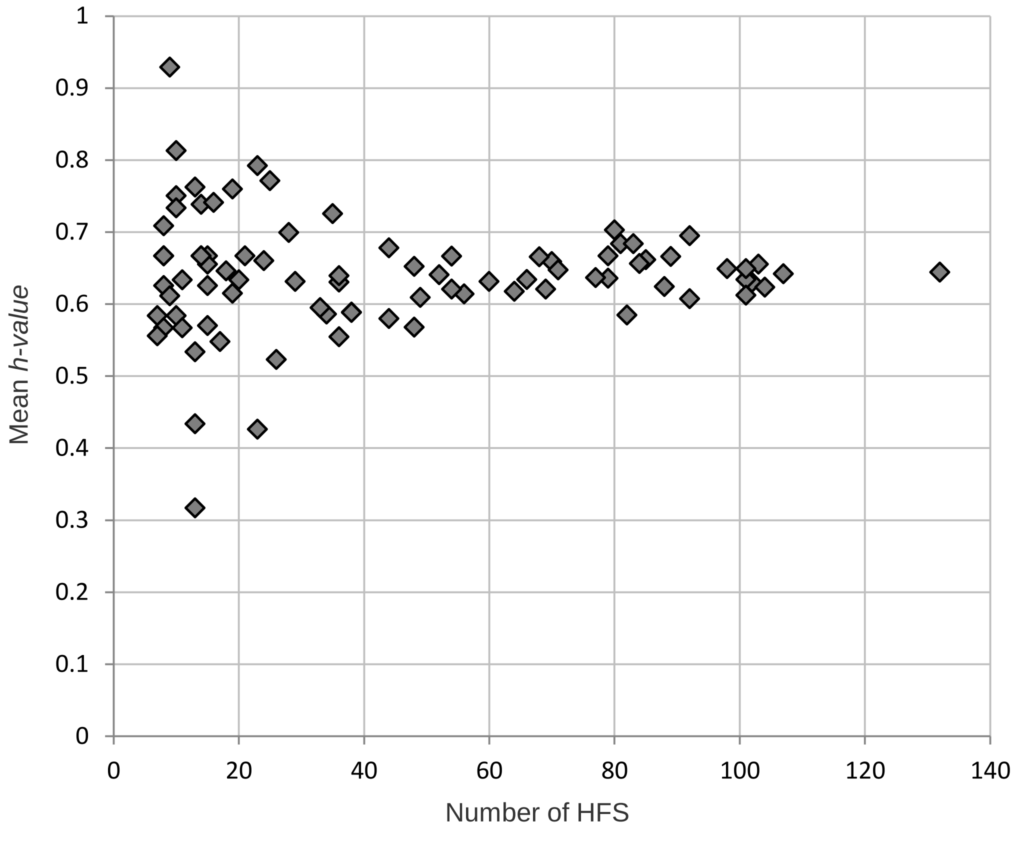

1
0.9
0.8
0.7
0.6
0.5
0.4
0.3
0.2
0.1
0
Mean *h-value*
0
20
40
60
80
100
120
140
Number of HFS

Figure 19

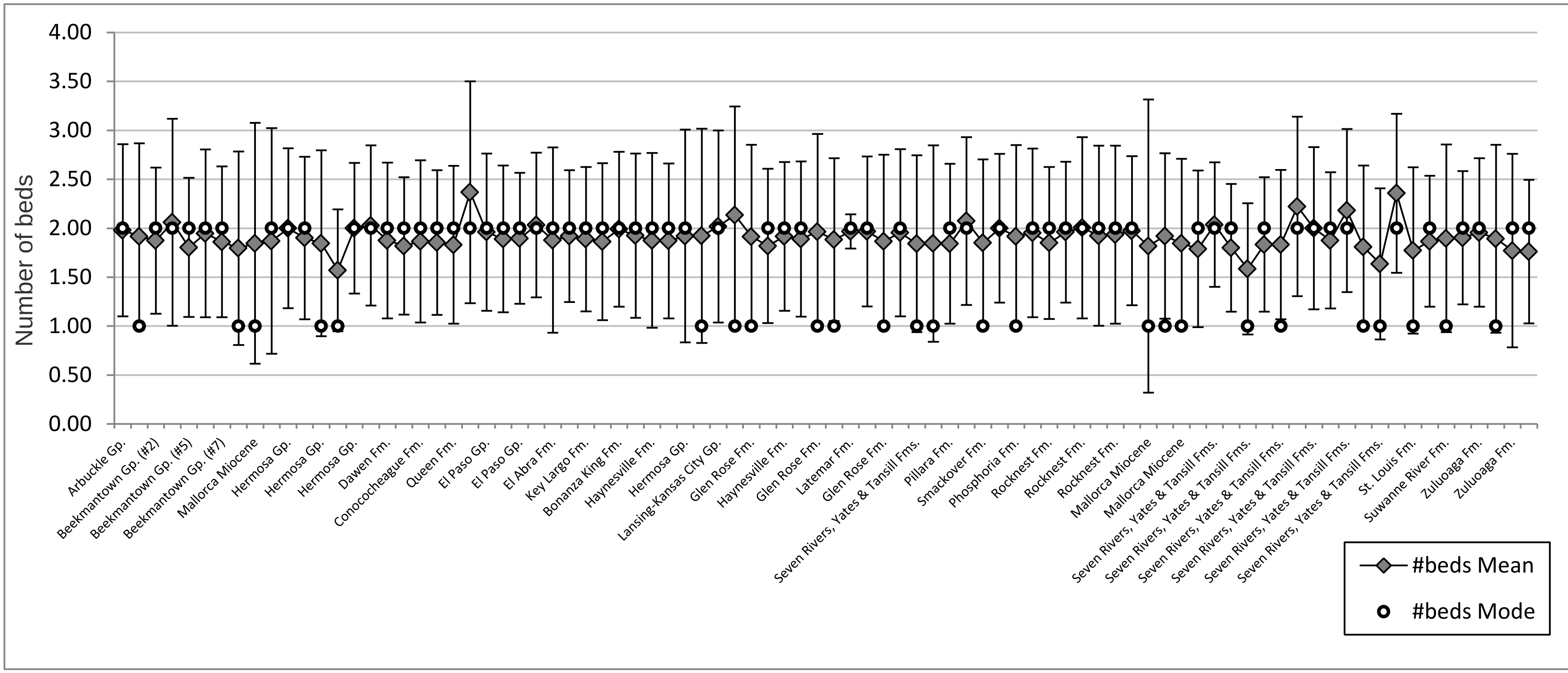
Number of beds
4.00
3.50
3.00
2.50
2.00
1.50
1.00
0.50
0.00
Arbuckle Gp.
Beekmantown Gp. (#2)
Beekmantown Gp. (#5)
Beekmantown Gp. (#7)
Mallorca Miocene
Hermosa Gp.
Hermosa Gp.
Hermosa Gp.
Dawen Fm.
Conococheague Fm.
Queen Fm.
El Paso Gp.
El Paso Gp.
El Abra Fm.
Key Largo Fm.
Bonanza King Fm.
Haynesville Fm.
Hermosa Gp.
Lansing-Kansas City Gp.
Glen Rose Fm.
Haynesville Fm.
Glen Rose Fm.
Latemar Fm.
Glen Rose Fm.
Seven Rivers, Yates & Tansill Fms.
Pillara Fm.
Smackover Fm.
Phosphoria Fm.
Rocknest Fm.
Rocknest Fm.
Rocknest Fm.
Mallorca Miocene
Mallorca Miocene
Seven Rivers, Yates & Tansill Fms.
Seven Rivers, Yates & Tansill Fms.
Seven Rivers, Yates & Tansill Fms.
Seven Rivers, Yates & Tansill Fms.
Seven Rivers, Yates & Tansill Fms.
St. Louis Fm.
Suwanne River Fm.
Zuluoaga Fm.
Zuluoaga Fm.
#beds Mean
#beds Mode

Table 1

Parameter	Step	Range	Iterations
High-frequency oscillation amplitude	10	0-100m	10
Intermediate-frequency oscillation amplitude	10	0-100m	10
Low-frequency oscillation amplitude	20	0-200m	10
Subsidence	100	10-900m	10
Carbonate production	500	50-5000m Ma^{-1}	11